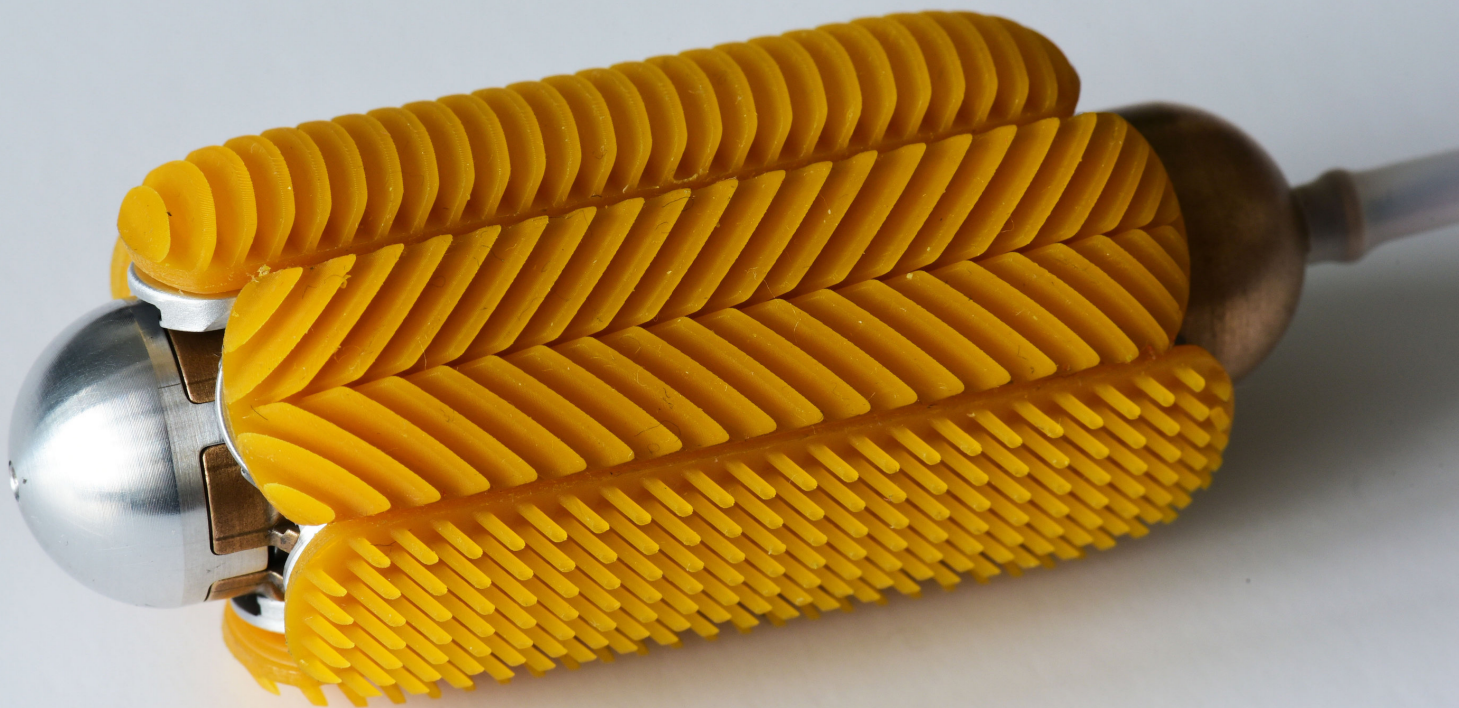


The design of a self-propelling mechanism for an endoluminal robot.

P. Posthoorn

Technische Universiteit Delft



The design of a self-propelling mechanism for an endoluminal robot.

by

P. Posthoorn

in partial fulfillment of the requirements for the degree of

Master of Science
in Mechanical Engineering

at the Delft University of Technology,
to be defended on Tuesday 17 January, 2017 at 15:00.

Student number:	1369571	
Thesis committee:	Prof. dr. ir. P. Breedveld	TU Delft, supervisor
	Dr. D. Dodou	TU Delft
	Ir. J.W. Spronck	TU Delft
	Ir. M. Scali	TU Delft

This thesis is confidential and cannot be made public until December 31, 2018.

An electronic version of this thesis is available at <http://repository.tudelft.nl/>.

Preface

For as long as I can remember I have been interested in how things work. From taking apart click-pens to disassembling washing machines, if it has moving parts it fascinates me and what better way to find out how a mechanism works than taking it apart and figuring out how to get it working again. This started at a young age and till this day I still find machines that are new to me and I want to figure out what makes them do what they do. This is what drove me to start a study in Mechanical Engineering, a broad study where you learn about all kinds of mechanisms from surgical instruments to combustion engines and from mechanical calculators to hydroelectric power generators.

Halfway through my master it was time to find a graduation topic. At our faculty many different intestine inspection devices have been designed in the past, and recently a group designed a steerable needle that can pull itself into a tissue. I asked the professor of my master track, Paul Breedveld, if the propulsion mechanism used in the needle could be used to create a self-propelling intestine robot; his response was that I had found my graduation topic: *"The design of a self-propelling mechanism for an endoluminal robot"*. This report is the final submission for my master thesis about this topic, to obtain the degree of Master of Science in Mechanical Engineering in the track Biomechanical Design specializing in Biologically Inspired Technology at the Delft University of Technology.

The design, manufacturing and testing involved with my graduation was a larger project than I anticipated and I would like to thank everyone who made this possible. First I want to thank my parents for raising me in an environment where I could discover where my interests lie and supporting me during my entire education. A big thanks goes out to Professor Paul Breedveld for giving me the freedom to design a completely new mechanism, for providing me with the opportunity to build a very nice prototype and for all feedback and support during my graduation project. Next I want to thank Henny van der Ster and Menno Lageweg at DEMO for converting my designs to a beautiful working prototype. I am also grateful for the feedback and support I received from my other supervisors: Dimitra Dodou, Marta Scali and Gerwin Smit. Last but not least I want to show my appreciation to my family and friends who supported me over the years during my time here in Delft.

Thanks for making this happen.

*Perry Posthoorn
Delft, January 2017*

CONTENTS		Appendix A: Experiment 1 data	20	
I	Introduction	3	Appendix B: Production drawings	20
	I-A Introduction to colonoscopy	3		
	I-B Current endoluminal devices	3		
	I-C Bio-Inspiration	5		
	I-D Problem definition	5		
	I-E Goal	5		
	I-F Outline	6		
II	From ovipositor to concept design	6		
	II-A Design requirements	6		
	II-B Working principle	6		
	II-C Concept design	8		
	II-D 3D printed proof-of-principle	8		
III	From concept design to final design	8		
	III-A Rotor	9		
	III-B Frame	9		
	III-C Cap	9		
	III-D Material	9		
	III-E Slider connection	9		
	III-F Ball bearings	9		
	III-G Number of sliders	9		
	III-H General shape	10		
	III-I Additional parts: 3D printed textures	10		
IV	From final design to prototype	11		
	IV-A Rotor and motor	11		
	IV-B Frame	11		
	IV-C Cap	12		
	IV-D Slider	12		
	IV-E 3D textures	12		
	IV-F Full assembly	12		
	IV-G Final prototype	12		
V	Experiments	14		
	V-A Experiment 1: Plastic tubes	14		
	V-B Experiment 2: Pig intestine	15		
VI	Results	15		
	VI-A Results experiment 1a: Without 3D textures in plastic tube	15		
	VI-B Results experiment 1b: With 3D textures in a plastic tube	15		
	VI-C Results experiment 2: With 3D textures in pig intestine	15		
VII	Discussion	16		
VIII	Future research	16		
	VIII-A 3D textures improvements	16		
	VIII-B Mechanism improvements	16		
	VIII-C Possible solutions	17		
	VIII-D Impression of redesign	17		
IX	Conclusion	18		
	References	18		

The design of a self-propelling mechanism for an endoluminal robot

Perry Posthoorn

Abstract—Current endoscopic devices cause great discomfort to the patient because they need to be pushed from outside the patient to manoeuvre through the intestine. Self-propelling endoscopic concepts have been proposed, but these cause unnecessary trauma to the patient or are unable to travel to the end of the large intestine and back. This study proposes a new design for a self-propelling endoluminal robot, based on the propulsion method found in the ovipositor of a wasp. The wasp uses multiple sliding segments to insert a needle into the bark of a tree. The robot in this study uses multiple segments to propel the device through the intestine. Only one segment moves forward at any given time, while the other segments are stationary with respect to the surrounding tissue. A rotating cam driven by a single motor actuates the segments. First a proof-of-principle design is 3D printed to prove that the mechanism is valid and then a working prototype is designed and produced. The prototype was tested in different plastic tubes and a porcine intestine.

Index Terms—Self-propelling, endoscope, robot, colon.

I. INTRODUCTION

A. Introduction to colonoscopy

CANCER in the colon or rectum, also colorectal cancer, is the third most common form of cancer in men and the second in women, with an estimated 1.4 million cases of cancer occurred worldwide in 2012 [1]. In the same year a total of 693,900 deaths were caused by colorectal cancer, accounting for 8 % of all cancer deaths. Colonoscopy, inspection of the colon, can reduce these numbers. A recent study carried out in the United Kingdom reported a reduction of colorectal cancer incidence by 33 % and mortality by 43% with a one-time screening between 55 and 64 years of age [2].

Colonoscopy is usually carried out with a colonoscope (Figure 1), a long and flexible tubular device with a steerable tip that contains a camera and light source to inspect the inside of the colonic wall. A colonoscopist inserts the device into the rectum of a patient and advances the colonoscope approximately 1.5m through the large intestine. Even though the tip of the device is steerable it is hard to control the shape of the entire device. The large intestine is a tubular organ with multiple bends and consisting of a soft tissue as shown in Figure 2. The wall of the intestine is not smooth but looks like connected bulbs. The inside of the colon is covered with a mucus layer, which makes generating friction a challenge. When the colonoscopist pushes the device forward it can hit a corner or bulb in the intestine and buckle. This causes strain on the colonic wall and surrounding tissue, which can cause pain and cramps to the patient.



Fig. 1: Illustration of conventional colonoscope. [3]

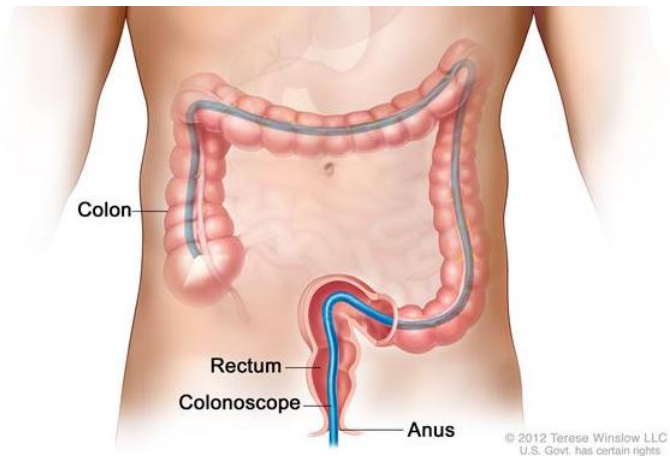


Fig. 2: Illustration of conventional colonoscopy. The colonoscope is pushed through the large intestine by the colonoscopist. [4]

B. Current endoluminal devices

The buckling of the colonoscope can be solved by generating a pulling force at the tip of the device, which will pull the device through the colon. To achieve this, friction between the tip of the device and the colonic wall is necessary. Several approaches to this problem were found in literature.

Chen et al. [5] designed a wireless self-propelling micro biopsy endoscope that uses expansion and contraction to move itself through the colon (Figure 3). The robot uses soft

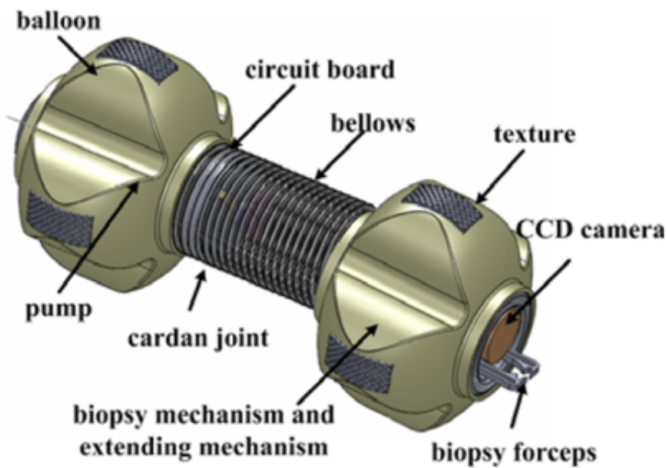


Fig. 3: Expanding-extending endoscopic robot by Chen et al. [5].

balloons at the front and rear that can be inflated and deflated individually, and the middle part of the robot consists of a bellows that can extend and contract. When moving from left to right the propulsion works as follows: The initial state has both balloons expanded and the bellows contracted. The right balloon then deflates, followed by the bellows extending which moves the right balloon to the right. The right balloon is then inflated, and the left balloon is deflated, followed by the bellows contracting which moves the left balloon to the right. The left balloon can now be inflated, and at this point the robot has the same configuration as at the start of the motion, but translated to the right. Chen et al.'s prototype had a diameter of 20mm at deflated state and a contracted length of 75mm. The prototype was tested in-vitro in a porcine intestine.

At Delft University of Technology multiple colonoscopy devices have been designed. A Gearwheel Device was designed by Ronald Root [6], shown in Figure 4. This device uses two rings with 12 gear wheels each driven by a single motor and battery incorporated in the device. The gearwheels were used to generate friction with the intestinal walls, but during an in-vitro test in a porcine intestine these gearwheels were unable to generate enough grip to move the device forward through the colon. It was assumed that the gearwheels were unable to penetrate the mucus layer that covers the inside of the intestine. Using larger teeth on the gearwheels to overcome this problem imposes the risk of the device damaging the intestine.

Another way to generate friction with the colonic wall is with mucoadhesive films. This is a special kind of adhesive tape that is able to stick to the mucus layer on the inside of the intestine. Research in this direction has been carried out at Delft University of Technology [7]. Figure 5 shows a design that uses these mucoadhesive films stored inside the device. In-vitro test in porcine colon showed it was difficult to create a device with enough power to drive the films and at the same time have enough storage capacity for these films to traverse through the entire large intestine. Another disadvantage of this design is that it can only propel itself in one direction.

A colonoscope that can propel itself through the large intestine without external forces and that can propel itself in

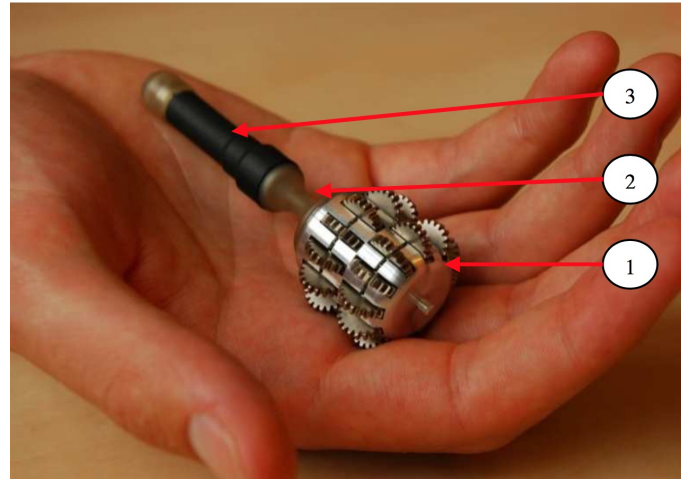


Fig. 4: Gearwheel Device by R. Root. The device consists of two rings each containing 12 outward facing gearwheels (1), these rings are flexibly connected (2) to an electric motor (3). [6]



Fig. 5: Two pictures of a device that can pull a colonoscope through the colon using mucoadhesive films. The top picture shows the inside of the device where the tape is stored and motors and transmission are housed. The bottom picture shows the full device compared to an AA battery.



Fig. 6: *Apocrypta Westwoodi* wasp inserting its ovipositor, picture by Lakshminath Kundanati [8]

two directions without damaging surrounding tissue would be an ideal replacement for colonoscopes currently used. Designs found in literature do not provide all these properties. Some can move in both directions but cause damage to the colon while others preserve the intestinal wall but are only able to move in one direction and need to be pulled out by a lead wire, which is uncomfortable for the patient.

C. Bio-Inspiration

Nature already found a solution for the insertion of a device into a material or lumen without pushing from the outside. Several species of parasitic wasps (e.g. *Megarhyssa* Nortoni, Braconidae, *Apocrypta Westwoodi* (Figure 6)) present a needle-like structure, called ovipositor [10]. The ovipositor, used to insert eggs into the bark of a tree, extends from the last abdominal segment of the wasp and consists of three long segments that slide along each other (Figure 7). Two narrower segments are connected to a wider segment, which transports the eggs. The segments are connected by means of a tongue and groove mechanism that ensures the segments do not separate when inserted. Serrations at the tip of the ovipositor ensure no slip occurs. By sliding the individual segments with respect to each other the ovipositor is advanced into the bark of the tree.

The working principle behind the propulsion mechanism of the wasp is based on the fact that multiple stationary segments generate enough static friction to overcome the static and dynamic friction needed to push one moving segment forward. This propulsion mechanism has already inspired the design of a needle with low net push force at Delft University of Technology [11]. This device consists of multiple segments, each driven by an individual linear actuator and is placed on a low friction cart. The segments are inserted into a gelatine substrate, then the segments are moved forward one after another and this 'pulls' the segments into the gelatine (Figure 8).

D. Problem definition

An endoscopic device that has an internal propulsion mechanism that does not rely on external forces would reduce patient

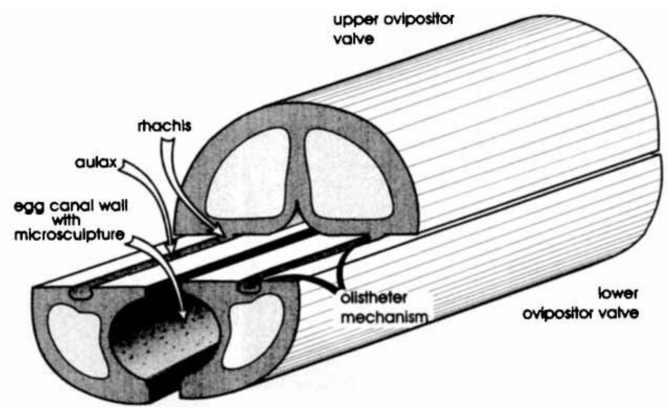


Fig. 7: Schematic drawing of the Braconidae wasp ovipositor [10]. Three segments are connected by T-grooves (rhachis) and in the center the egg canal is visible.

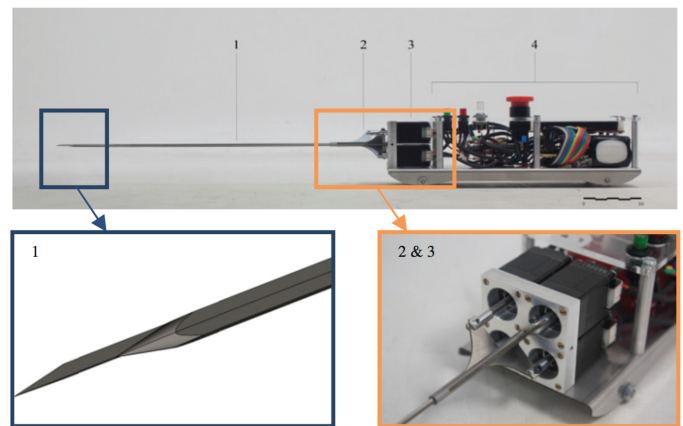


Fig. 8: Needle insertion device inspired by the wasp [11] showing the needle (1), needle assembly (2), linear actuator assembly (3), and the low friction cart with driving electronics (4).

discomfort and increase the ease of use for the operator. The principle where multiple stationary segments generate enough friction to move a single segment forward has already been applied to needle insertion but it is unknown whether this principle is usable for the propulsion of an endoscopic device.

E. Goal

The goal of this research is to design a propulsion mechanism for a self-propelling (independent of external forces) endoluminal robot inspired by the principle found in the wasp. This mechanism should be able to move in two directions and it cannot cause damage to the surrounding tissue.

As a secondary goal it would be valuable if the design could be used as a test platform to investigate the friction generated by different textures with the colonic wall.

Thus in this paper we will introduce the design of a self-propelling, ovipositor-based device and present a prototype with a modular design that can be used to test different textures to optimize the friction with the colonic wall.

F. Outline

The structure of the remainder of this paper is as follows. In chapter II the design process from the mechanism found in the wasp to a first concept design is described. In this chapter a clear description of the mechanism is given and illustrated, followed by the design and pictures of a 3D printed prototype. Chapter III shows the changes and improvements that are needed to create a viable design for an endoluminal robot. In chapter IV the design of this robot is illustrated with rendered drawings used for the production of a physical prototype. This chapter ends with several pictures of a working prototype. Chapter V describes the two different experiments that were carried out to verify the performance of the prototype in plastic tubes and a porcine colon. The results of these experiments are described in chapter VI. In chapter VII the experimental results are discussed and in chapter VIII a number of improvements are suggested for future research. These suggestions are inspired by the knowledge gained during the experiments. An artist's impression containing several of these improvements is given at the end of this chapter. Finally chapter IX summarizes the conclusions drawn from this research. At the end of this paper is an appendix with the production drawings of the physical prototype.

II. FROM OVIPOSITOR TO CONCEPT DESIGN

A. Design requirements

The device must be able to propel itself through a human colon, but for testing purposes we will use a pig colon, which is anatomically comparable with a human colon. The colon consists of a thin, flexible tissue in the form of a tube with a mucus layer on the inside. Our goal is to use the friction between the colonic wall and the surface of the device to move forward, thus the device should fill the cross section as much as possible. This can be achieved best by using a device with a cylindrical shape that has the same diameter as the inside of the colon. In the case of a European human large intestine this diameter is 23-36mm [12].

The colon consists of straight parts and corners and the device should be able to follow this anatomy without problems. A single compact device is desired and thus the length of the device is limited to 70mm.

When the colon is inspected it is empty and thus folded together. To ensure the device can move through the colon without damaging it, a rounded-off front and back of the device would be optimal.

Powering and controlling the actuators used for moving the device can be done via a wire-connection from outside the patient or wireless. The first option always ensures that the device has power to move in and out of the patient, while with the second option problems with signal emission/reception can occur. Having a flexible wire going from the device to outside the patient will not influence the performance of the device and is not more uncomfortable to the patient.

With this in mind the following requirements for the prototype were specified:

- Self-propelling: propulsion through a lumen without any force acting on the device from outside of the lumen.
- Powered and controlled by a wire to outside the patient.
- Forward and backward propulsion
- Maximum diameter: 30mm
- Maximum length: 70mm

B. Working principle

The foundation of the principle found in the wasp is that the friction on multiple stationary segments is enough to move one moving segment further into the substrate. The wasp achieves this with only three segments but the principle is valid for more segments as well.

Because the ovipositor of the wasp needs to cut and move through a substrate it must be sharp and as thin as possible and thus the actuators (i.e. muscles) are positioned outside the ovipositor, inside the body of the wasp. Our device will be used to travel through a lumen and because only a power line can go to outside the patient, all actuators and mechanics to move the segments should be incorporated in one compact design. To achieve this the design of the propulsion mechanism must be altered. The segments do not need to be thin and sharp but only have to make contact with the surroundings on the outside of the device. Thus the segments can slide along the sides of the a device with a cylindrical shape and the actuation mechanism contained within this cylinder.

The wasp uses individual muscles to actuate each segment. A mechanical design that uses an individual actuator per segment is possible, however this makes the control of the device more complex and might not be space efficient. Since the motion is repetitive and periodic a single actuator for the entire mechanism is preferred.

A direct conversion of the principle found in the wasp to a general motion for a mechanism is to let each individual segment slide forward and when all segments are extended the rest of the robot can also move forward to reset the mechanism. A schematic illustration of this algorithm is shown in Figure 9. The illustration shows the four different states of the system. The first state shows the initial position of the segments with respect to the frame of the device. In state 2 the first segment moves forward with respect to the frame and thus slides along the wall of the lumen the device is in. State 3 shows the second segment moving forward and in state 4 the third segment moves forward. In state 1 we see the frame has moved forward with respect to the segments and all segments remained at the same position with respect to the surroundings. At this point the entire mechanism has the same shape as the initial state but is now advanced a certain distance through the lumen.

The vertical distance from each segment to the centre of the frame is different per state for each segment, this is indicated by the red surface in Figure 10. We can plot this distance over time for every segment to get the path each segment follows with respect to the frame. These paths are shown in Figure 11. It is clear that each segment needs a unique path. This could make the design of the mechanism quite complex and could be a problem for the maximum dimensions if the number of segments is to be increased.

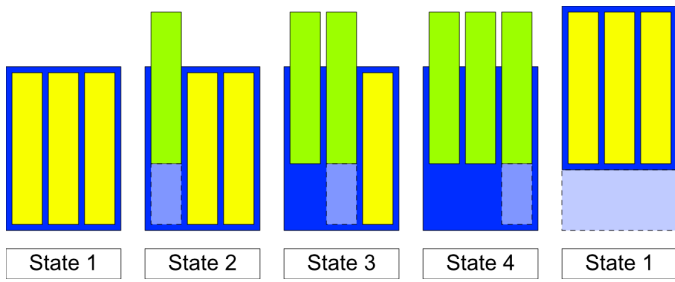


Fig. 9: Schematic illustration of a propulsion algorithm inspired by the wasp. The yellow and green rectangles represent segments that can move forward individually and the blue rectangle represents the frame of the device. State 1: Starting position, all segments and the frame are at the same position. State 2: The first segment moves forward. State 3: The second segment moves forward. State 4: The third and last segment moves forward. State 5: The frame moves forward, the entire mechanism has now progressed a certain distance forward with respect to the surroundings.

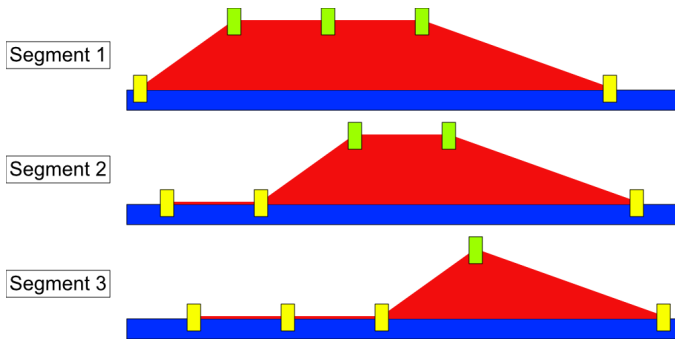


Fig. 10: The blue line indicates the centre of the frame. The yellow rectangles represent the initial vertical position with respect to the frame. The green rectangles represent the moved position of the segments with respect to the frame. The red surface indicates the vertical distance from each segment to the frame.

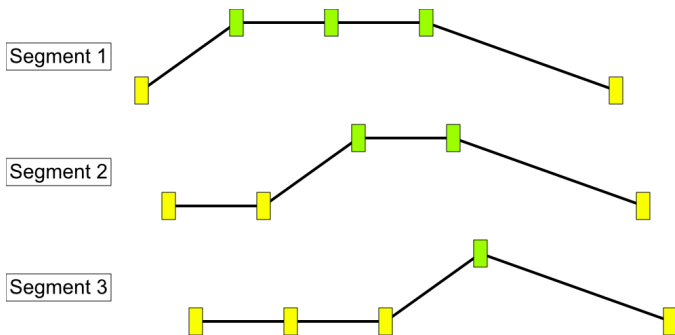


Fig. 11: The yellow rectangles represent the initial vertical position with respect to the frame. The green rectangles represent the moved position of the segments with respect to the frame. The black lines show the path that each segment follows with respect to the frame during the motion of the mechanism.

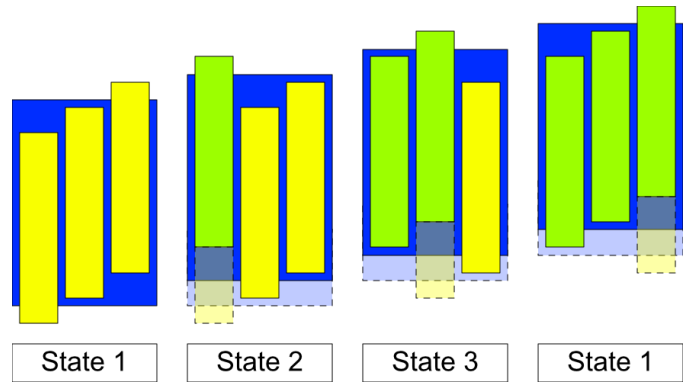


Fig. 12: Schematic illustration of the optimized propulsion algorithm. The yellow and green rectangles represent segments that can move forward individually and the blue rectangle represents the frame of the device. In each state one segment moves forward with respect to the other segments and thus slides along the wall of the lumen at the same time the frame also moves forward with respect to the two stationary segments and surroundings.

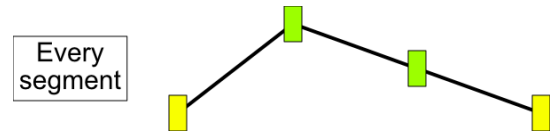


Fig. 13: The yellow rectangles represent a single slider in the three different states. The black line shows the path this segment follows with respect to the frame. Every segment can use this same path with a time delay between the different segments.

To allow more segments in a tighter space this general algorithm can be optimized so that each segment does not need its own individual path. Instead of moving the frame forward after all segments have been advanced, the frame can move forward a little with every segment that moves forward. This gives the frame a constant velocity with respect to the surroundings. An optimized algorithm based on this idea is shown in Figure 12.

In this figure we see the state of the system at three different time instances. Every step a single segment moves forward while the other segments stay stationary with respect to the surroundings. Meanwhile the frame also moves forward a little with every step. In this algorithm every segment follows the same path with respect to the frame, albeit there is a delay in between the individual segments. This path is illustrated in Figure 13.

Summarizing, we started with an algorithm that needed multiple actuators or a complex mechanism to actuate each segment individually resulting in discrete propulsion. This algorithm was converted to a mechanism that can actuate all segments with a single actuator using a mechanism that ensures each segment follows the same path resulting in continuous propulsion of the device.

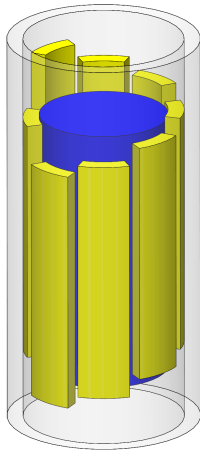


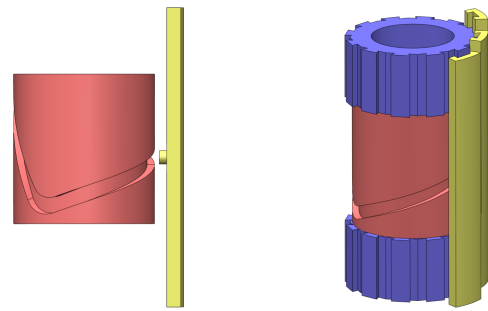
Fig. 14: 3D representation of the algorithm from Figure 12. Yellow sliding segments surround the blue cylinder representing the frame. The device is shown inside a transparent tube that represents the environment through which the device must propel itself.

C. Concept design

The working principle shown in the previous section was converted to a functioning 3D mechanism. As stated in the requirements, a cylindrical shape is preferred as this ensures good contact with the intestinal wall. We can convert the algorithm shown in Figure 12 to a 3D shape as shown in Figure 14, where a central blue cylinder represents the frame and around it are in this example eight yellow segments that can slide up and down. The path shown in Figure 13 can be wrapped around this cylinder and the segments attached to the outside of the cylinder can follow this path in longitudinal direction when the cylinder is rotated around its own axis. An easy method to ensure each segment follows the path is to deboss the path into the cylinder forming a groove and extend a pin from the centre of each segment into this groove. The result is a rotating cylinder with an axial cam that is followed by a pin connected to each segment (Figure 15a).

The segments need to be attached to the device in such a way that they can slide forward and backward freely but still stay attached to the device. This can be achieved by a dovetail or T-groove connection. To ensure these guides provide enough support the segments are attached to these guides at the top and bottom of the device. This means the frame needs to pass through the rotating cylinder. The result is shown in Figure 15b.

The design choices discussed above were combined to create the proof of principle design shown in Figure 15b. This design uses a rotating cam to move a maximum of 12 segments. Because this proof of principle design was produced using 3D printing a dovetail connection was chosen to attach the segments to the frame of the device. Creating a T-groove using 3D printing resulted in a weak, flexible T-groove that did not provide enough support to slide the segments along. The dovetail design did create a strong connection while still allowing the parts to slide along each other.



(a) A cylinder with a cam that drives a segment via a pin. (b) A cylinder with a cam that rotates around a frame. In this example three segments are attached to the frame with dovetail connections. Each segment is actuated by a pin that fits inside the cam in the cylinder.

Fig. 15: Two illustrations of cylindrical cams with sliding segments.

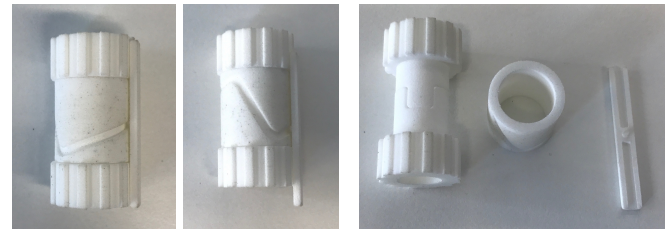


Fig. 16: 3D Printed proof-of-principle prototype.

D. 3D printed proof-of-principle

The 3D printed prototype was used to verify the working of the rotating cam and sliding segments. Pictures of the prototype are shown in Figure 16.

When holding the blue frame between index finger and thumb, the cylinder with cam can be rotated with the other hand to move the sliding segments up and down. The proof-of-principle showed that for the shallow angle of the cam the prototype performed very well. But the steep angle of the cam made it impossible to move the segment in the other direction without also directly pushing forward on the segment. Much of this can be attributed to the large friction coefficient of the 3D printed material (Shapeways Strong and Flexible [13]). In the final design this friction should be minimized and the angle of the cam should be decreased to ensure a smooth operation of the mechanism.

III. FROM CONCEPT DESIGN TO FINAL DESIGN

To verify the proposed propulsion algorithm a fully functional prototype needs to be designed. The concept design shown in the previous section needs to be analysed in different aspects. A motor needs to be incorporated and the frame can be redesigned to ensure assembly is not too difficult. The concept design had open ends, but the final design needs to be a closed system to ensure the motor stays clean. Some sort of cap should be designed to close the ends of the device. The concept design was 3D printed using Shapeways Strong and

Flexible plastic and as indicated this resulted in too much friction. A more durable and smoother material should be selected. The sliders need to be redesigned to ensure they can be manufactured. In this chapter we will discuss the changes and improvements we made on the design.

A. Rotor

The concept design was turned by hand but the final design needs to incorporate a motor. In the concept design the rotating cylinder (which will be called *rotor*) is on the outside of the frame. This makes it difficult to get a transmission from the motor to the rotor. It would be easier if the rotor were placed inside the frame directly onto the motor. This means that there needs to be room to connect the sliding segments (called *sliders* from this point on) to the rotor through the frame. Because the sliders only move in axial direction with respect to the frame we can make slots in the frame through which the sliders can connect to the cam in the rotor.

B. Frame

In the concept design the frame passed through the rotor and the sliders were supported at both sides of the rotor to prevent tilting. In the final design the rotor is inside the frame and thus the frame can be constructed as a single part with guiding rails for the sliders along the entire length of the frame. This minimizes the chances of tilt for the sliders and also simplifies manufacturing and assembly. The motor and rotor can be inserted in the frame from the top; this allows the bottom of the frame to be closed.

C. Cap

To ensure no dirt enters the device, some kind of cap needs to be designed on top of the frame that can be attached after the motor and rotor are inserted. The cap is inserted into the frame and held on by clamping pressure between the two parts. During manufacturing and testing it might be useful to be able to rotate the rotor by hand. To simplify this the rotor should protrude from the frame and the cap can cover this protrusion. Thus, when the cap is removed, the rotor can be rotated between two fingers.

D. Material

The concept design was manufactured using 3D printing because this is a fast and low cost method to create a proof-of-concept. For the final design a more durable material is desired and friction should be minimised. The majority of the parts will be manufactured using a form of CNC machining. A strong material that can be easily machined and is often used for medical applications is Aluminium 7075. When two parts of this material slide along each other galling can occur. To prevent this all sliding surfaces within the mechanism should consist of one part Aluminium 7075 and one part a material that has a low friction with Aluminium 7075. For this second material we chose to use bronze. This material is strong enough but minimises processing time.

The mechanism contains three different sliding interactions. The rotor rotates inside the frame, the sliders slide along the frame and a part of the slider slides through the cam in the rotor. The last sliding surface can be replaced by a ball bearing which converts the sliding contact into a rolling contact. This leaves only two sliding surfaces because now the rotor and slider do not have a sliding surface between them, thus we can use the same material for both components. As Aluminium 7075 is stronger than bronze, and the sliders will be the thinnest parts of the mechanism, we chose to use Aluminium 7075 for the sliders and rotor. Consequentially the frame is made out of bronze.

E. Slider connection

The dovetail design used to attach the sliders to the frame in the concept design was chosen because this shape is easy to manufacture using a 3D printer. The final design will be made on a CNC machine and a precise dovetail is very difficult to realise on a CNC machine. But in contrast to 3D printing, machining makes it possible to create a very precise T-groove, provided that a small enough milling bit is available. T-bits with a thickness of the 'top bar of the T' in the range of tenths of millimetres can be found. We chose to use a T-groove with a thickness of 0.5mm, this leaves enough material to create a strong connection and these milling bits are reasonably easy to obtain.

F. Ball bearings

To keep the size of the device to a minimum the ball bearings should be as small as possible. The smallest ball bearings have an outer diameter of 1.5mm and inside diameter of 0.5mm [14], but these are not readily available. The smallest ball bearings that are easy to obtain have an outer diameter of 3mm [15]. This is small enough for our design and these bearings have an inside diameter of 1mm which allows us to use a thicker axle that is better capable of supporting the load from the rotor, inside the frame, to the slider, outside the frame.

G. Number of sliders

The working principle of our mechanism relies on stationary surfaces generating more friction force than the force that is needed to advance one surface. This principle works with a minimum of three surfaces: two stationary and one advancing at any time. The more surfaces used, the more force the stationary surfaces generate with respect to the sliding surface. But using more surfaces also means more parts, which increases manufacturing cost and assembly time.

Because we chose to use ball bearings with an outer diameter of 3mm there is a hard maximum on the number of segments that fit in our design. The requirement for the outside diameter of the device is 30mm. We estimate that each slider including possible textures will be 6mm thick, which means the rotating cylinder can have a maximum outer diameter of 18mm. The ball bearings will move inside a debossed cam inside this cylinder and the ball bearings have a thickness

of 1mm. To avoid contact between the ball bearings there should be a space of at least 0.2mm between the bearings at their closest point, 8mm from the centre of the cylinder. With these numbers we can calculate the maximum number of ball bearings that will fit this design, and thus the maximum number of sliders. The circumference where the ball bearings are closest to each other is $\pi * 16 = 50.2mm$. Each ball bearing will need $3mm \text{ } \odot + 0.2mm \text{ spacing} = 3.2mm$ so the maximum number of segments is $50.2 \div 3.2 = 15.7$ which means no more than 15 segments will fit in our design.

The dimensions of the cam driving the bearings lead to the exact number of segments. As it is determined that one segment should move while the rest are stationary there are two variables that influence the number of segments: the angle of the part of the cam that moves a segment forward and the distance this segment moves forward with each stroke. To overcome flexibility and elastic deformation in the surroundings we estimate a stroke of at least 5mm is necessary. The 3D printed proof-of-principle from the previous chapter showed the angle of the cam should not be too high. In Figure 17 the stroke per number of segment is shown for three different angles, 20°, 30° and 40° and the desired minimal stroke of 5mm is also indicated. For the three different angles (20°, 30° and 40°) the maximum number of segments is 3, 6 and 8. A lower number of segments leads to a larger stroke, but will also decrease the ration between moving and stationary segments, which might decrease the performance. To ensure the motor will be able to rotate the cylinder a large angle should be avoided. With this in mind we chose to use an angle of 30° and a total of six segments. This results in a stroke of 5.1mm and the frame of the device will have a symmetrical, hexagonal shape, which has the advantage of being simpler to manufacture than a device with an uneven number of segments.

H. General shape

The intestine through which the device must propel itself will lay flat inside the abdomen. This means the device must open the intestine to be able to move itself forward. To make this easier both ends of the device are given a spherical shape. Because the cap on the front of the device needs to be removable and a sphere is hard to grasp, the tip of the cap is provided with an M2 threaded hole. A bolt can be inserted to remove the cap and when the device is in use a setscrew can be inserted to ensure no dirt enters the device.

On the rear end of the device there must be an exit hole for the power cable. This cable will be surrounded with a silicone tube to prevent it from getting entangled. This silicone tube should be fastened to the device to ensure an accidental pull on the cable does not result in the cable detaching from the motor. This is achieved by creating a protrusion around the cable hole at the end of the device to which the silicone tube can be fastened.

I. Additional parts: 3D printed textures

The proposed mechanism works in two directions and independent of the texture of the outside of the device, but as

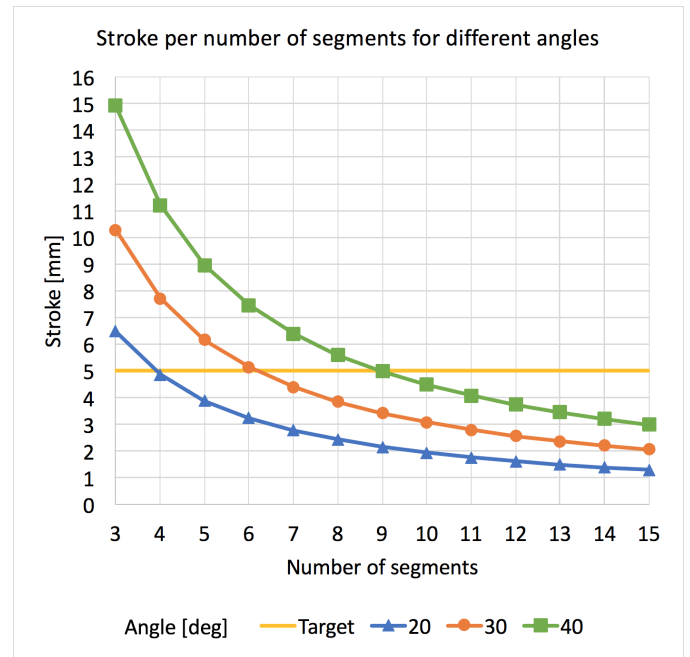


Fig. 17: The stroke per rotation is shown per number of segments for different angles. The yellow line represents the target stroke of 5mm and the blue (triangle), orange (circle) and green (square) lines show the stroke for different number of segments for maximum cam angles of 20°, 30° and 40° respectively.

a side objective we would like to achieve a maximum forward speed by optimizing the design of the texture on the outside of the device that interacts with the intestinal wall. We could create different sliders with different textures but this would be costly because each slider needs a T-groove and ball bearing. An alternative is to design the sliders in such a way that 3D printed texture can be attached to each slider. These textures can then be replaced easily. This allows us to create multiple 3D textures, which can then be interchanged during testing. It is also faster and cheaper to experiment with different textures because the cost of 3D printing these parts are much lower than machining an entire slider. Thus, the design of the textures can be optimised.

We want as much space as possible for the 3D textures so the thickness of the aluminium sliders is kept to a minimum. The T-groove will be about 1mm thick and the rest of the slider will also be 1mm. This results in a total thickness of 2mm and leaves about 6mm of thickness for the 3D textures. To ensure the 3D printed textures align on the sliders two recesses are created in the sliders. The inside of the 3D textures will have two protrusions that fit in these recesses.

As a control test, we will use a solid texture with a smooth surface on the outside. Furthermore, we will test three different 3D textures. Because the sliders only interact with the intestinal wall in axial direction it makes sense to create a two-dimensional texture. The first texture consists of flaps extending out of the device in radial direction. The second texture contains shallow pillars that allow more room for the mucus layer to get into the texture. This ensures the pillars

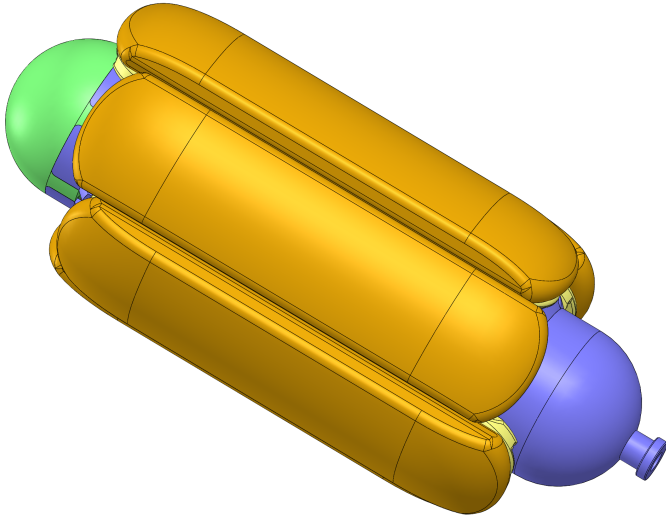


Fig. 18: Complete assembly of the prototype.

can have a direct interaction with the intestinal wall. The third texture is inspired by the design of tractor tires. This texture uses the same flaps as the first texture but now they are positioned in a V-shaped pattern in the longitudinal direction of the slider. This should increase the grip when the slider is stationary with respect to the colonic wall, but also allow better mucus drainage when the slider is pushed forward along the tissue.

Because we want to optimize the speed in forward direction all protrusions are created with an angle of 60° to the base of the slider. This will ensure the colonic wall can easily pass over the texture when the slider moves forward, but when the slider moves backward the protrusions can bend outward to increase the grip on the colonic wall.

IV. FROM FINAL DESIGN TO PROTOTYPE

The changes and improvements in the previous section led to the final design shown in Figure 18. We see the ends of the device are closed except for the cable opening at the end. The device has a much more rounded shape than what we saw in the concept design. This ensures a smooth contact with the colonic wall. In this section, we will show all details of the prototype.

A. Rotor and motor

The heart of the final design consists of the motor and rotor. The motor used in the final design consists of a high rpm DC motor [16] with a fixed gearbox with a ratio of 1:16 [17]. In Figure 19 the rotor is shown. We can see the path discussed in Section II-C resulted in a cam wrapped around the outside of the cylinder. This cam will guide the bearings that drive the sliding segments. In the final design the maximum angle of the cam is XX° and the length of the steep part of the cam is $XX\text{mm}$. Together this results in a stroke, the axial travel distance of each slider per rotation, of $XX\text{mm}$. To accommodate the shape of the motor but still keep the outside dimensions of the device to a minimum the top of the rotor

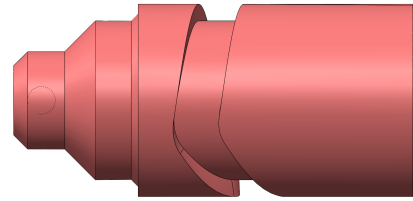


Fig. 19: Rotor

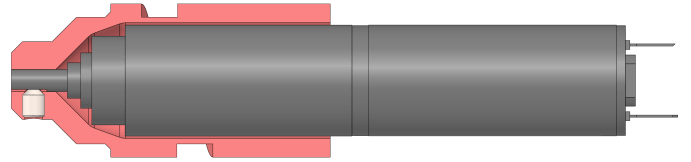


Fig. 20: Rotor on motor.

has a stepped shape. A combination of the motor and rotor is shown in Figure 20. The rotor fits tight around the motor and is secured to the axle with a setscrew.

B. Frame

The frame of the device holds all moving parts together. As shown in Figure 21 the six T-grooves are distributed around the outside of the frame to support the sliding segments. The slots in the T-groove to accommodate the ball bearing axle reaching the rotor can be found at the front of the frame. At the bottom of the frame we find the exit hole for the power cable leading to the motor. This exit hole has a ring around the end to connect a silicon tube that protects the power cable.

In Figure 22 we can see how the rotor and motor fit inside the frame and how setscrews keep the motor in place.

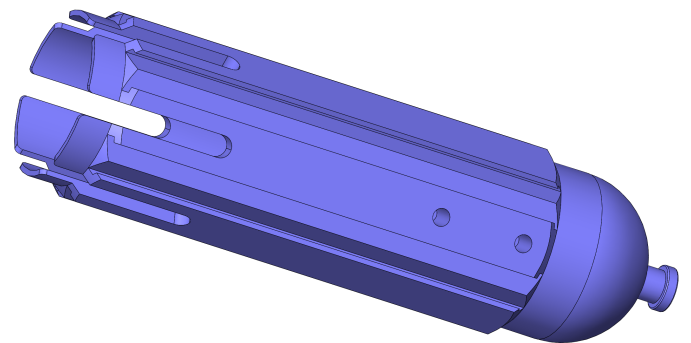


Fig. 21: Frame

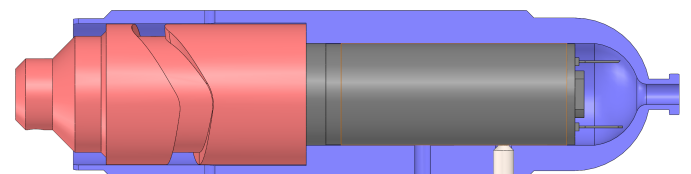


Fig. 22: Frame with motor and rotor.

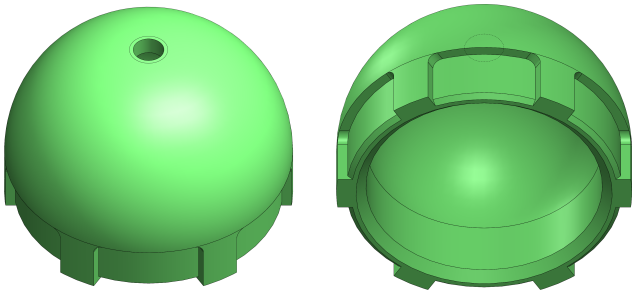


Fig. 23: The cap of the device shown from above and below.

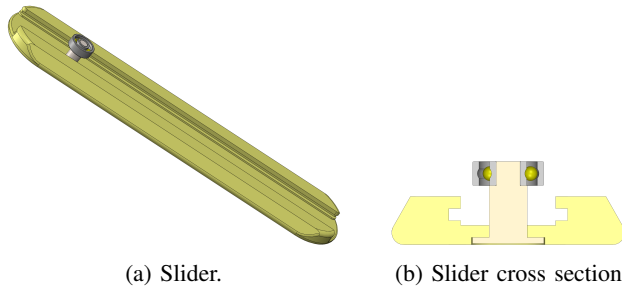


Fig. 24: Slider subassembly with the axle and ball bearing

C. Cap

The cap that closes the frame is depicted in Figure 23. The cap is a hemisphere to ensure it can move through the colon easily. But this also makes it hard to remove without pliers that would damage it. Thus, there is a hole in the centre of the cap into which a threaded bolt could be inserted. This bolt can be used to pull the cap off the frame and when the device is used a short setscrew can be screwed into it to ensure no dirt enters the device.

D. Slider

Each sliding segment consists of three parts: the slider with T-groove, a ball bearing and an axle connecting these two parts. In Figure 24a we can see them all together and Figure 24b contains a cross section that shows how these parts fit into each other. The axle is glued in the slider and the ball bearing is then press-fitted onto the axle.

E. 3D textures

The design of the four different textures is shown in Figure 25. With all textures the device will have an outside diameter of 28mm and a homogeneous outer surface. The smooth surface is shown in Figure 25a. This smooth surface will function as a control test with no texture at all. All non-smooth surfaces have a texture that is under an angle of 60° with the surface of the slider. Because of the fine details in the textures the easiest manufacturing technique to make the textures is 3D printing.

In Figure 25b we find the first textured surface. The pillars have a diameter of 0.75mm, using the AB-flex material this results in flexible pillars that can be easily pushed down to take the form of the surroundings but they are stiff enough so

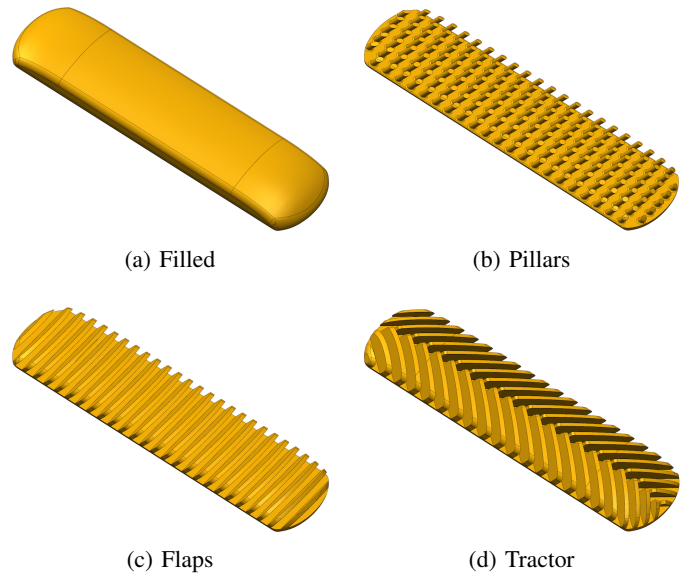


Fig. 25: The average and standard deviation of critical parameters: Region R4

that they do not flex beyond 90° when the slider slides along the intestinal wall.

Two textures were designed with a texture in the form of flaps. The first, shown in Figure 25b uses straight flaps with a thickness of 0.5mm. This results in roughly the same flexibility as the pillars structure when pressed down. The second flap texture is inspired by tractor tires. The flaps are under a 45° angle with each other. This should increase the grip but also allow the mucus to flow out of the gaps between the flaps when the texture slides along the colonic wall.

F. Full assembly

The final design is shown in Figure 18. All parts are combined in a compact cylindrically shaped device. The exploded view in Figure 26 shows how all parts fit together. In this view the sliders are shown as a complete sub-assembly. The ball bearing is on the axle connected to the slider and the smooth 3D texture is also attached to the slider. In Figure 27 a cross section of the device shows the tight fit between the different components. Only one of the three setscrews used to secure the motor to the frame is visible in this cross section.

Production drawings of all parts and (sub) assemblies were created and are available in Appendix B. All sizes and dimensions can be found in these drawings.

G. Final prototype

The rotor, frame, cap, sliders and bearing axles were all manufactured by DEMO at Delft University of Technology using a five-axis milling machine. The 3D textures were also manufactured by DEMO. They were printed using an EnvisionTec's Perfactory 4 Mini XL with ERM 3D printer [18] using EnvisionTec's AB-flex [19], a flexible ABS-like material. This resulted in textures with flexible protrusions on a rigid base.

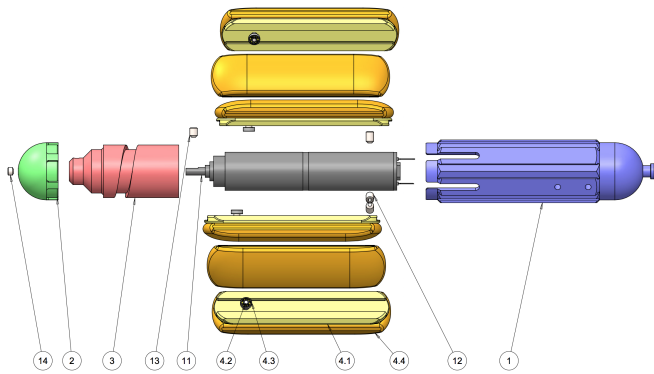


Fig. 26: Exploded view of the prototype. Parts: frame (1), cap (2), rotor (3), motor (11), slider (4.1), slider bearing (4.3), bearing axle (4.2), smooth 3D texture (4.4), set screws (12,13,14).

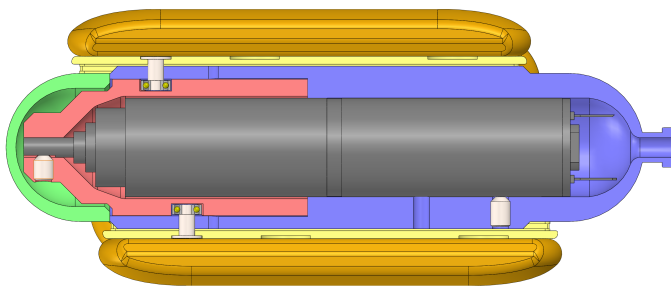


Fig. 27: Cross section of the prototype.

The machined parts, together with the motor, are shown in an exploded view layout in Figure 29. The ball bearings are already on their axles which are connected to the sliders.

The assembly without 3D textures is shown in Figure 30. In this setup, the device measures 18.3-20.5mm in diameter and 67.5mm in length (64.5mm without the cable protrusion). A shaft was inserted through the cable hole and fastened to the rotor with a setscrew to manually turn the rotor. This allowed us to feel the force required to power the system. After some initial rotations, the rotor turned very smooth and we were confident the selected motor would be able to power

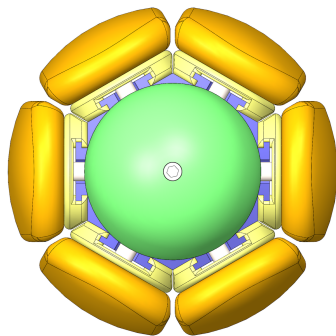


Fig. 28: Front view of the prototype, the circular perimeter with space in between the 3D textures is visible as well as the T-grooves supporting the sliders.



Fig. 29: Exploded view of the prototype.



Fig. 30: Assembled prototype.

the device. In Figure 31 the 3D textures are attached to the final prototype and the motor is built in the device. For size comparison an AA battery is shown next to the prototype. With the 3D textures attached, the prototype has in an outside diameter of 28mm with a circular cross section. The front view shown in Figure 32 highlights the T-grooves used to attach the sliders to the frame. And finally Figure 33 shows the prototype held in a hand.

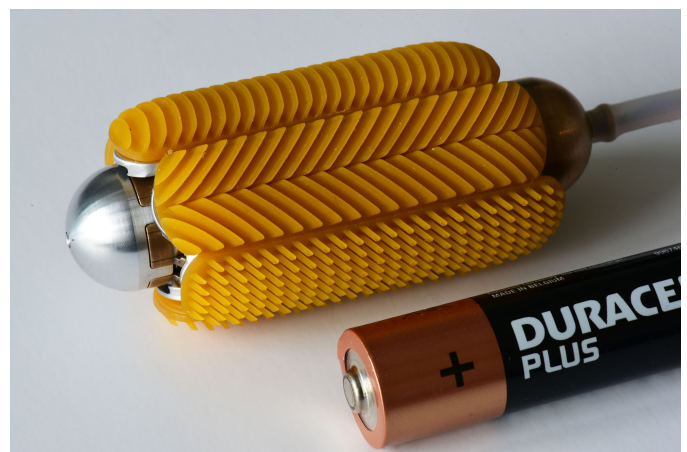


Fig. 31: Assembled prototype with 3D textures compared to a standard AA battery. The three different textures are visible, from top to bottom: straight flaps, tractor flaps and pillars. On the right side of the picture the silicone tube protecting the power cable and attached to the protrusion is visible.

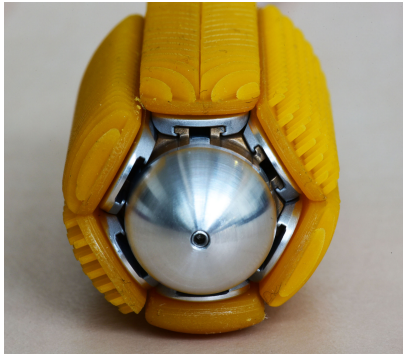


Fig. 32: Front view of the assembled prototype with 3D textures.

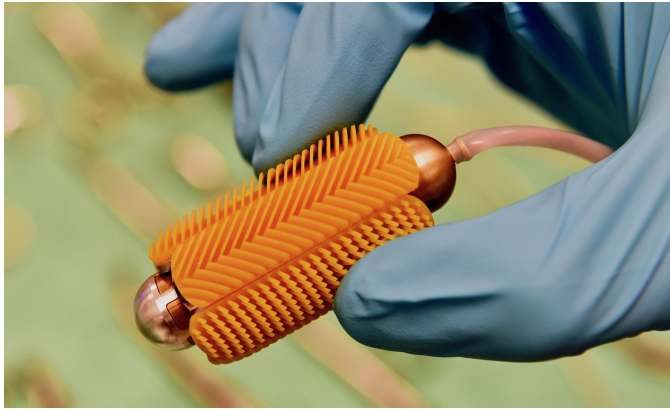


Fig. 33: The assembled prototype with 3D textures held in hand.

V. EXPERIMENTS

The propulsion mechanism designed and produced in the previous sections was verified using two different experiments. The first experiment tested the operation and performance of the device. This was done in plastic tubing materials that fit the outside diameter of the device with or without the 3D textures. In the second experiment the device was tested inside a large intestine of a pig.

A. Experiment 1: Plastic tubes

First the device was tested without attaching any 3D textures to the sliders. This meant the tube should have an inside diameter between 18.5mm and 21.5mm, these are the widths of the prototype measured on the flat sides and corners respectively. Additionally, it would help when the material of the tube is somewhat flexible so it can shape to the hexagonal cross section of the device. The tubing we found that fits these criteria is a central heating pipe isolation material. This material is used in The Netherlands to isolate water pipes for central heating with an outer diameter of 15mm. The inner diameter of the isolation material is approximately 19mm, and it fits snug around the prototype. A piece of this tube was used for experiment 1a with a length of 330mm. The device is shown in a short piece of this tube in Figure 34.

The second test in a plastic tube was done with 3D textures attached to the sliders. To create a tube with an inside diameter

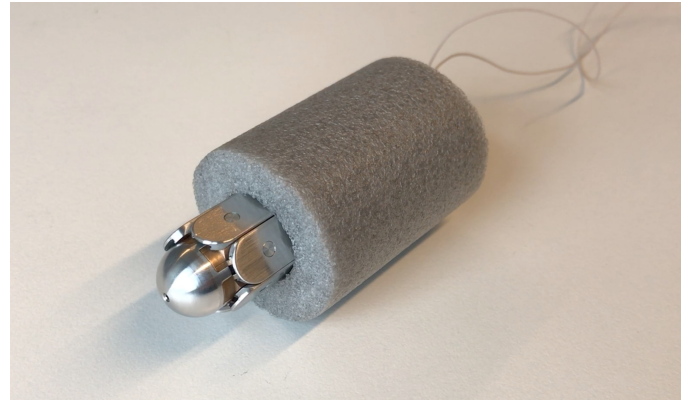


Fig. 34: Assembled prototype without 3D textures inside a short piece of the isolation tube.

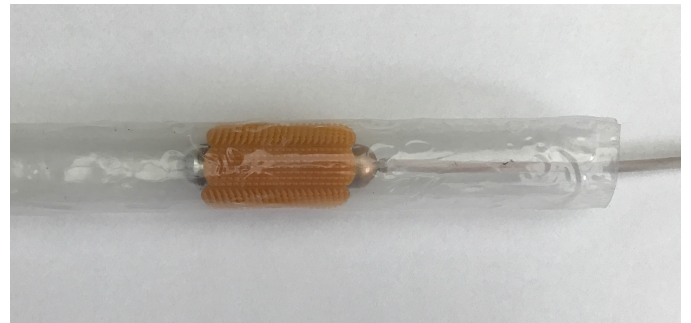


Fig. 35: Assembled prototype with 3D textures with pillars inside the shrink tube.

of 28mm a heat-shrink tubing [20], with a diameter before shrinking of 44mm, was shrunken around a solid rod with an outside diameter of 28mm. A piece of this tube with a length of 350mm was used for experiment 1b. The device with pillar 3D textures attached is shown inside this tube in Figure 35.

Both tests focused on the actual operation and performance of the device. The motor in the device was powered with the maximum allowable voltage of 12V to achieve the highest possible speed. The power was turned on and off manually when the device travelled a distance of approximately 270mm to ensure the device had full contact with the tube. The velocity of the device moving through the tubes was measured and the amount of slip was determined. Slip was defined as the measured velocity divided by a 'potential velocity'. The potential velocity was calculated by multiplying the measured rotational speed of the motor with the stroke of one slider.

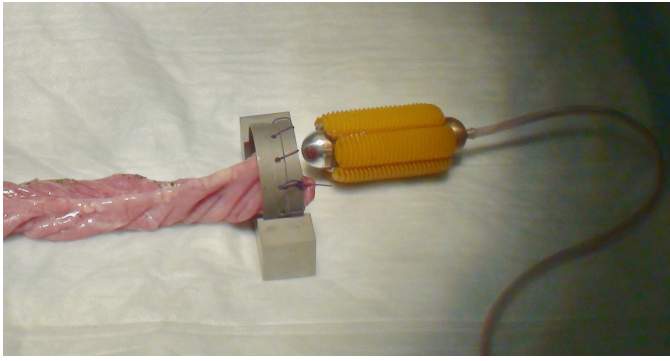


Fig. 36: Assembled prototype with 3D textures with straight flaps and the pig colon attached to a ring to keep it open.

This stroke was measured in advance as being 5.2mm. The device was tested in both forward and backward direction and each experiment was repeated three times for a total of 12 measurements in plastic tubes.

B. Experiment 2: Pig intestine

In the second experiment a large intestine of a pig was used to test the performance of the device. This ex-vivo experiment was carried out at the Academic Medical Center in Amsterdam at the department of Experimental Surgery. Different pieces of colon were used with varying diameters.

The experiment was performed on an operating table using the available operating lights. A video camera on a tripod was used to record the experiments. The pig intestine was prepared by cleaning the inside and outside, and then an opening ring was sutured to one end of the intestine to keep it open. Next the prepared intestine was placed on the operating table and weights were used to position the intestine in a U shape. Then the appropriate 3D textures were attached to the prototype and the device was positioned in the opening of the colon.

Finally, the camera was started and the power on the motor was turned on to perform and record the experiment. After each experiment the device was disassembled, cleaned and reassembled with different 3D textures.

The test set-up is shown in Figure 36. Here we can see the device with straight flap 3D textures attached to it and displayed next to a piece of colon that is attached to an opening ring.

VI. RESULTS

A. Results experiment 1a: Without 3D textures in plastic tube

The first verification of the working of the prototype was done in an isolation tube. As indicated the experiment was repeated three times and on average the prototype moved 271.3mm through the tube in 10.0s, this results in an average speed of 27.1mm/s. In this time the motor made 65 rotations. With the predetermined stroke of the device of 5.2mm per rotation a theoretical distance of $65 * 5.2mm = 338mm$ would have been possible without any slip. Thus, the slip in this experiment can be calculated as the measured average distance divided by the theoretical distance, which results in a slip factor of: $271.3mm \div 338mm = 0.80$.

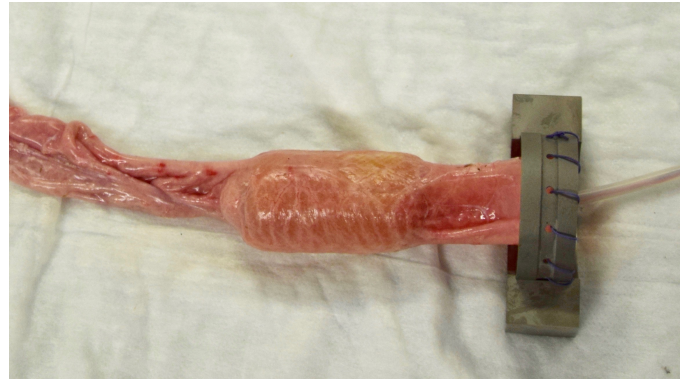


Fig. 37: Assembled prototype with 3D textures inside the colon.

The performance in backward direction was also tested; this resulted in an average speed of 25.9mm/s and a slip factor of 0.81.

B. Results experiment 1b: With 3D textures in a plastic tube

During the tests with 3D textures the prototype travelled an average distance of 265.3mm through the shrink tube in 5.3s with the pillar shaped 3D texture attached to the sliders. This resulted in an average speed of 50.1mm/s. The motor made 52 rotations resulting in a theoretical distance of 270.4mm. The slip factor then becomes $265.3mm \div 270.4mm = 0.98$.

The same experiment was done in backward direction and this resulted in an average speed of 52.3mm/s with a slip factor of 0.99.

All measurement data obtained during Experiment 1 can be found in the table in Appendix A

C. Results experiment 2: With 3D textures in pig intestine

The first attempt used a piece of colon with a relatively small diameter. When the motor was turned on all sliders moved as expected but the device did not advance through the colon. The 3D textures gripped the colonic wall very well and the tissue was so flexible that it moved along with each slider. Because the forward moving slider did not slip along the colonic wall the device did not propel itself forward at all. In Figure 37 the prototype is shown inside the colon.

The test was repeated with a piece of colon with a large diameter and this did not have any effect. The four different 3D printed textures were tested in both the small and larger diameter colon but none of them allowed the device to propel itself through the colon.

When a small amount of force was applied to the device by pushing on the silicon cable sleeve the device did start moving slowly. The device also started moving forward when the colon was squeezed by hand and more force was applied at the rear of the device than at the front of the device. The behaviour of the device was also tested with the colon held in an angle of about 45 degrees, hanging freely and only supported by the ring. In this test the prototype was able to move itself forward with the support of gravity.

VII. DISCUSSION

Inspired by biology, a propulsion mechanism was designed that requires no external force to propel a device through a lumen. The foundation of the mechanism is that multiple stationary segments create enough friction to slide one moving segment forward. A single motor was used to rotate a cylinder with a cam on the outside. This cam moves sliding segments forward and backward. This mechanism was used to build a working prototype of an electrically driven endoluminal robot. The final prototype was used in two experiments to validate the designed mechanism.

The first experiment showed that the prototype worked very well in two different plastic tubes. In experiment 1a the device moved through foam-like material without 3D textures attached to the sliders. The speed was comparable in both forward and backward direction; the marginally lower speed in backward direction can be attributed to motor properties. The slip factor was almost equal in both directions; this was to be expected because there was no direction dependent texture attached to the device. In experiment 1b 3D textures were attached to the sliding segments and the device propelled itself through a thin walled shrink-tube. Forward moving velocity was again almost equal to backward velocity, but in this case the backward velocity was a little bit higher. With a slip factor of 0.98 almost no slip occurred, indicating the 3D texture provided a very good contact with the tube.

The experiments in plastic tubes showed that the proposed mechanism and prototype are able to propel through a tubular environment without external forces. The experiment in the isolation tube showed that without direction dependent textures the device is able to move in both directions with comparable velocity and a moderate amount of slip. In the experiment with a shrink-tube it was shown that the direction dependent 3D textures allowed the device to move through the tube with almost no slip. But because the performance was again comparable in both directions this might be an effect of the interaction between the 3D texture material and shrink-tube material instead of an effect of the direction dependent 3D texture.

In the second experiment the device was tested in the colon of a pig. With and without any of the different 3D textures the results were the same: the device was unable to propel itself through the colon without external force. The intestinal wall was so flexible that it flexed between the different sliders.

The main difference between the two experiments is that in the first experiment the plastic tubes are stiff but in the second experiment the pig colon is quite flexible. We learned that, while in the plastic tubes all stationary elements provide support to push one segment sliding forward along the wall of the lumen, in the flexible colon only the interaction between two sliders moving in opposite direction is of importance. It is at this interaction where the slider moving forward should slide along the colonic wall, but the other sliders should stay stationary with respect to the colonic wall. In our design, especially with the 3D textures attached there is a part of the colonic wall, between two sliders, that is not touching the sliders. This provides a dampening effect to the sliding of

the forward moving segment along the colonic wall. We also saw that the friction between the 3D textures and colonic wall was always so large that no slip ever occurred. The expected direction dependent friction was not present. This resulted in the colonic wall being stuck to the sliders at all times and thus the colon always moved along with all the segments around the device.

To summarize, there are two main reasons why the prototype did not propel itself through the pig colon. The first reason is the empty space between the different segments (this can be seen in Figure 28). This space allows the colon to flex between the sliders that move in opposite directions. The second reason is that the 3D textures were not direction dependent enough. At all times the colonic wall was stuck to the texture. The colonic wall should only be stuck to the texture when it is stationary, and the texture should be able to slide along the colonic wall when it is moved forward.

VIII. FUTURE RESEARCH

The limitations of our design discussed in the previous section inspired us to propose several directions in which the design can be improved to ensure the mechanism will work inside a colon.

A. 3D textures improvements

The current 3D textures are homogeneous over their entire surface and there is space between the different sliders where there is no contact with the colonic wall. To minimize the flexing of the colonic wall between two sliders the 3D textures should be as close to each other as possible.

The homogeneous surface has the result that the point of engagement is located in the middle of the surface of the 3D texture. This increases the negative effect of the flexible tissue. To ensure the forward moving slider actually slides along the colonic wall, the engagement point should ideally be located at the sides of the slider.

Although the current 3D textures were designed with direction dependent friction in mind we think the design can be further improved to ensure this behaviour. A design where the textures extend when the slider moves back and contract when the sliders moves forward would improve the direction dependency. This will increase the grip in one direction and decrease it in the other direction, and by extending the texture on one slider the colonic wall will be lifted and decrease the contact with the adjacent slider.

B. Mechanism improvements

The improvements shown in the previous section can all be applied to the current prototype. But we also found different aspects where the mechanical design of the device can be improved. Currently the stroke of each slider is 5.2mm. As the experiments showed this works very well in plastic tubes, but in the flexible colon this stroke is insufficient. A larger stroke would allow the slider to move far enough forward to ensure the surface slides along the colonic wall. There is a limit to how much the stroke can be increased. This depends

on the number of sliders and maximum angle of the cam in the rotor. In the current design the angle of the cam was chosen on the safe side to ensure the motor would be able to actuate the sliders. We found that the motor has more than enough power for our purpose and thus this angle can be increased to create a larger stroke.

In Section III-G we argued a design with six sliders would be optimal. With the knowledge gathered during the experiments we can make a better assessment of the different variables that influence the number of sliders. The motor used in our experiment had enough power to drive the mechanism with a relatively low cam-angle of 30° , thus we think a redesign with a higher cam-angle of 40° would be viable. The targeted stroke length of 5mm proved to be too small to overcome the flexing of the colonic wall and thus a redesign should focus on increasing the stroke length. We also saw that the ratio of stationary versus moving segments did not have a great impact and the interaction between two segments moving in opposing direction plays a much larger role in propelling the device forward. As shown in Figure 17 a larger stroke can be obtained by increasing the cam-angle as well as decreasing the number of segments. With the experience gained from our prototype we think both changes can be made to increase the stroke length to at least 9mm when using for example five sliders and a cam-angle of 40° .

A practical improvement can be made to achieve an easier assembly process. In the current design the axle of the ball bearing of each slider is glued into the slider and the ball bearing is pressed on this axle. This glue connection is fragile and made assembly a challenge. The axle can be held in place by the ball bearing when a small bushing is used as spacer between the ball bearing and slider.

C. Possible solutions

Shifting the engagement point to the side of the slider can be achieved by creating a protruding texture at the sides of the slider and leave the centre of the texture empty. This will cause the colonic wall to touch only at the intersection between two sliders and it will have no contact with the slider at the centre of the slider. This concept is illustrated by the cross section shown in Figure 38.

To achieve a better direction dependency, we designed two new textures to be used with the above-discussed design where only the sides of the sliders touch the colonic wall.

The first option is based on the Pillar design we already used. To increase the direction dependency the angle of the pillars with respect to the slider is lowered and the pillars are thinner to increase flexibility. This will cause the pillars to lay flat on each other when the slider moves forward, but the pillars will 'curl upward' when the slider moves backward and this will ensure a much larger difference in grip between two sliders moving in opposite directions. An illustration of this concept is shown in Figure 39.

The second option uses a structure that can best be described as inverted L shapes close to each other. When the slider moves forward the inverted L shapes form a smooth surface that can easily slide along the colonic wall. But when the slider moves

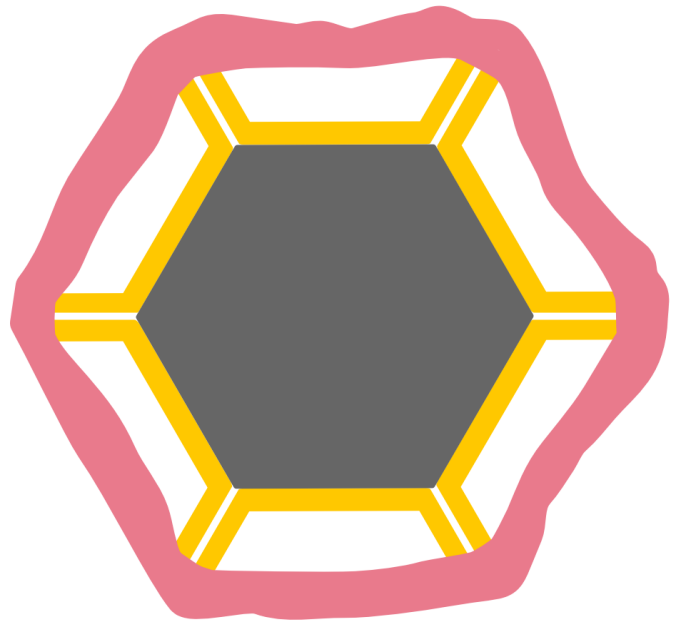


Fig. 38: Cross section of device with redesign 3D textures inside colon. The grey hexagon is the body of the device. The yellow lines represent the new 3D textures and colon is shown in pink. As shown the textures only touch the colonic wall at the side of the sliders. The centre of the textures is empty and the textures on different sliders are positioned close to each other.



Fig. 39: Concept design of improved angled pillars. In the top image the yellow slider moves to the right along the pink colonic wall; the texture forms a smooth surface. In the bottom image the slider moves to the left, creating a rough surface and increasing the height of the texture.

back the L shapes bend and form small hooks that create a rough surface that increases the grip on the colonic wall. This concept is illustrated in Figure 40.

D. Impression of redesign

A combination of a 3D texture with contact material only at the sides of each segment and the L shapes and new pillars is shown in the artist's impressions in Figure 41.

The improved texture with L shapes at the sides of the segments and the segments close to each other have been incorporated in a redesign shown in Figures 42 and 43.

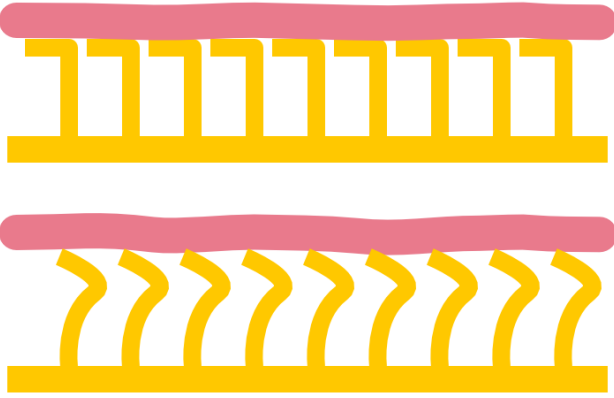
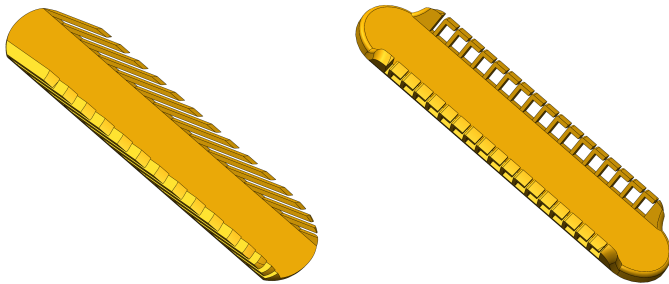


Fig. 40: Concept design of an inverted L shaped texture. In the top image the yellow slider moves to the right along the pink colonic wall; the texture forms a smooth surface. In the bottom image the slider moves to the left, creating a rough surface and increasing the height of the texture.



(a) Redesigned 3D texture with 'pins' on a low angle of 20° and only at the sides of the slider. (b) Redesigned 3D texture with inverted L shaped 'pins' and only at the sides of the slider.

Fig. 41: Two redesigned 3D textures

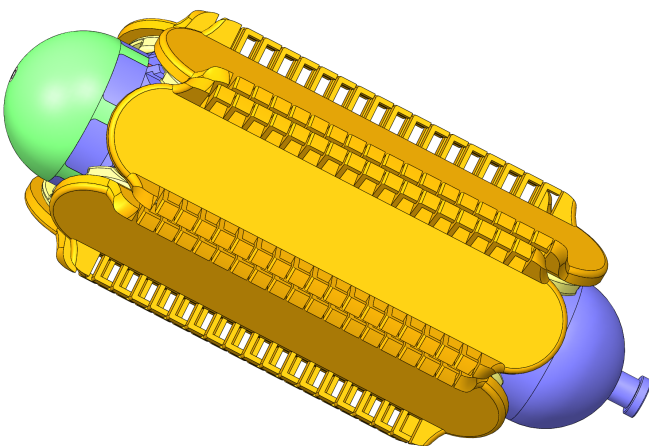


Fig. 42: A render of the assembly with the improved L-shaped 3D textures.

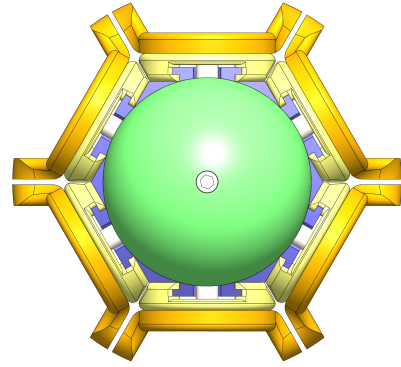


Fig. 43: A front view of the redesign. The different sliders are closer to each other than in the original design and the centre of each slider is empty.

IX. CONCLUSION

In this study a self-propelling mechanism inspired by a wasp ovipositor was designed. A working prototype powered by a single motor was produced within the required dimensions. Experiments with this prototype showed the mechanism works very well in plastic tubes. The device was able to move in two directions without external forces. A second experiment showed the current design does not yet work in a pig colon. In contrast to our expectations the forward moving slider was unable to slide along the colonic wall and instead the colonic wall moved along with the different sliders. This is caused by the flexibility of the colonic wall and the fact that the friction of the outside surface of the prototype was not direction dependent enough.

Several recommendations were made to improve the mechanism to ensure a new design will work as desired inside the colon. The stroke of a new design should be enlarged, for example by increasing the cam-angle driving the sliders and decreasing the number of sliders. The 3D textures should also be improved by ensuring that the main interaction with the colonic wall takes place at the sides of the slider. Furthermore the direction dependency of the 3D texture should be increased.

ACKNOWLEDGMENT

The authors would like to thank DEMO at TU Delft; especially Henny van der Ster for manufacturing the prototype and Menno Lageweg for producing the 3D printed textures. Furthermore the authors would like to thank the department of Experimental Surgery at the Academic Medical Center in Amsterdam, especially Goos Huijzer, for supplying space and material to test the prototype in a pig colon.

REFERENCES

- [1] American Cancer Society. *Global Cancer Facts & Figures 3rd Edition*. Atlanta: American Cancer Society, 2015.
- [2] Atkin WS, Edwards R, Kralj-Hans I, et al. *Once-only flexible sigmoidoscopy screening in prevention of colorectal cancer: a multicentre randomised controlled trial*. *Lancet*, 2010 May 8. 375(9726):162433.

- [3] Meditechtrade,
www.medtechtrade.com/en/equipment/colonoscope-10
- [4] Terese Winslow LLC. U.S. Government. 2012
- [5] W. Chen, G. Yan, H. Liu, P. Jiang, and Z. Wang, *Design of micro biopsy device for wireless autonomous endoscope*, Int. J. Precision Engineering Manufacturing, vol. 15, no. 11, pp. 23172325, 2014.
- [6] R. Root, *Colonic Locomotion: Development of the Muco Adhesive Device*, in BioMedical Engineering Delft: Delft University of Technology, 2008.
- [7] J. Mattheijer, *Design of a Rolling Propulsion Device to Pull a Conventional Colonoscope Through the Colon*, Delft University of Technology, 2009.
- [8] Apocrypta westwoodi image. www.sci-news.com/biology/science-fig-wasps-zinc-ovipositor-01951.html
- [9] Ahmed T, Zhang T, He K, Bai S, Wang Z *Sense organs on the ovipositor of Macrocentrus cingulum brischke (hymenoptera: braconidae); their probable role in stinging, oviposition and host selection process.*, J Asia Pacific Entomol, 2013 16:343348.
- [10] Rahman, M.H., Fitton, M.G., Quicke, D.L. *Ovipositor internal microsculpture in the braconidae (insecta, hymenoptera)*. Zool. Scr. 27, 319332 (1998)
- [11] T. Sprang, P. Breedveld, D. Dodou *Wasp-Inspired Needle Insertion with Low Net Push Force*, Conference on Biomimetic and Biohybrid Systems, Living Machines 2016: Biomimetic and Biohybrid Systems pp 307-318
- [12] D. A. Watters, A. N. Smith, M. A. Eastwood, K. C. Anderson, R. A. Elton, and J. W. Mugerwa, *Mechanical properties of the colon: comparison of the features of the African and European colon in vitro* Gut, vol. 26, pp. 384-92, Apr 1985.
- [13] Shapeways Strong and Flexible material,
www.shapeways.com/materials/strong-and-flexible-plastic
- [14] Smallest ball bearing,
www.nmbtc.com/technologies/worlds-smallest-ball-bearing/
- [15] SKF ball bearing,
www.skf.com/my/products/bearings-units-housings/ball-bearings/deep-groove-ball-bearings/stainless-steel-deep-groove-ball-bearings/single-row-stainless-steel/index.html?designation=W%20618%2F1
- [16] Maxon motor RE 10mm 1.5W, partnumber: 118400,
www.maxonmotor.nl/maxon/view/category/motor
- [17] Maxon planetary gearhead GP 10mm, partnumber: 218416, www.maxonmotor.nl/maxon/view/category/gear
- [18] EnvisionTec 3D Printer, envisiontec.com/3d-printers/perfactory-family/p4-mini-xl/
- [19] EnvisionTec AB-Flex material, envisiontec.com/3d-printing-materials/perfactory-materials/ab-flex/
- [20] Conrad Components 93014c87 Shrinktube Nominal 44mm www.conrad.nl/nl/conrad-components-93014c87-93014c87-krimpkous-zonder-lijm-transparant-nominale-voor-krimpen-44-mm-21-542044

TABLE I: Measurements from Experiment 1

Tube	Distance [mm]	Time [s]	Rotations	Theoretical Stroke [mm]	Theoretical Distance [mm]	Direction	Speed [mm/s]	Slip	Average Stroke
Shrinktube	265	5,4	52	5,2	270,4	Forward	49,1	0,98	5,1
Shrinktube	266	5,3	52	5,2	270,4	Forward	50,2	0,98	5,1
Shrinktube	265	5,2	52	5,2	270,4	Forward	51,0	0,98	5,1
Shrinktube	258	5,1	50	5,2	260,0	Backward	50,6	0,99	5,2
Shrinktube	259	4,9	50	5,2	260,0	Backward	52,9	1,00	5,2
Shrinktube	256	4,8	50	5,2	260,0	Backward	53,3	0,98	5,1
Isolation tube	270	9,92	65	5,2	338,0	Forward	27,2	0,80	4,2
Isolation tube	273	10,07	65	5,2	338,0	Forward	27,1	0,81	4,2
Isolation tube	271	9,99	65	5,2	338,0	Forward	27,1	0,80	4,2
Isolation tube	273	10,95	65	5,2	338,0	Backward	24,9	0,81	4,2
Isolation tube	272	10,32	65	5,2	338,0	Backward	26,4	0,80	4,2
Isolation tube	274	10,41	64	5,2	332,8	Backward	26,3	0,82	4,3

APPENDIX A

EXPERIMENT 1 DATA

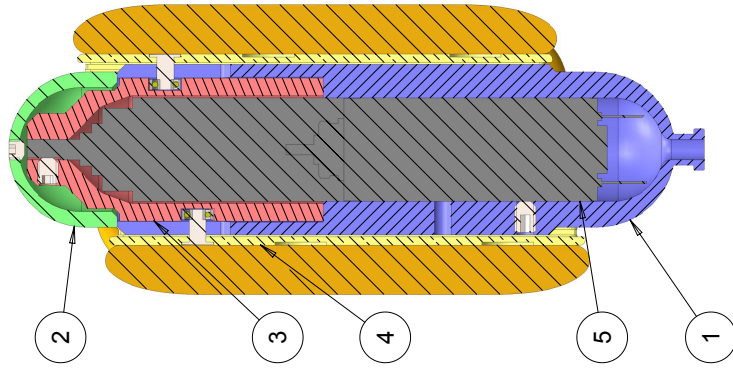
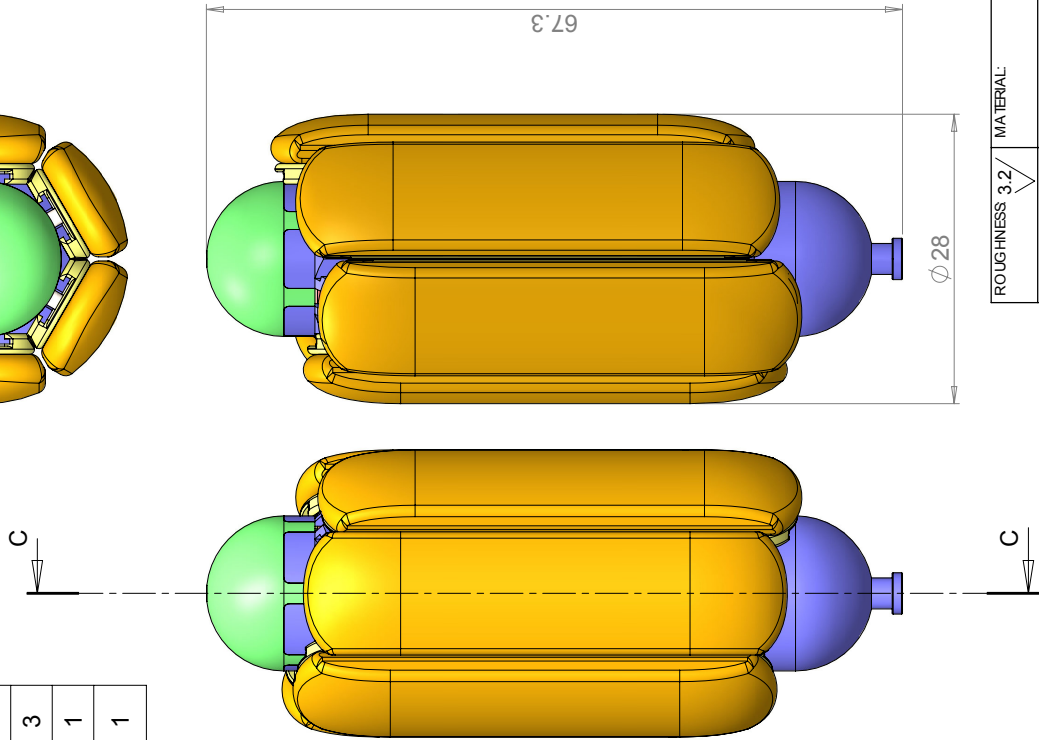
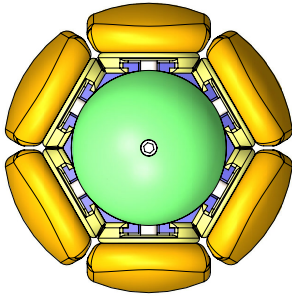
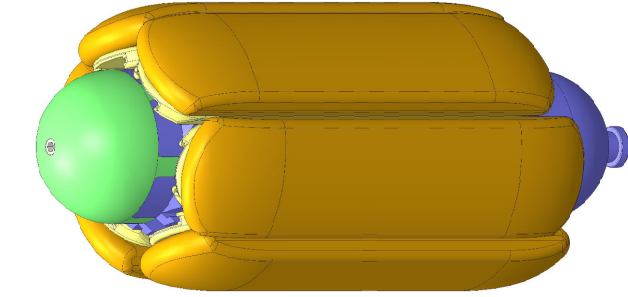
The measurement data gathered during Experiment 1 is visible in Table I. The first column shows the kind of tube used for the measurement. The following columns show the measured distance, time and number of rotations per experiment. The theoretical stroke is equal for all measurements as this is defined by the geometry of the prototype. Using the measured number of rotations and theoretical stroke the theoretical distance is calculated. The column labelled 'note' shows the direction in which the prototype moved through the tube. In the next column the speed is calculated by dividing the distance by the time for each measurement. The following column shows the slip factor. This is calculated as the measured distance divided by the theoretical distance. Finally the average stroke is shown. This is the measured distance divided by the number of rotations.

APPENDIX B

PRODUCTION DRAWINGS

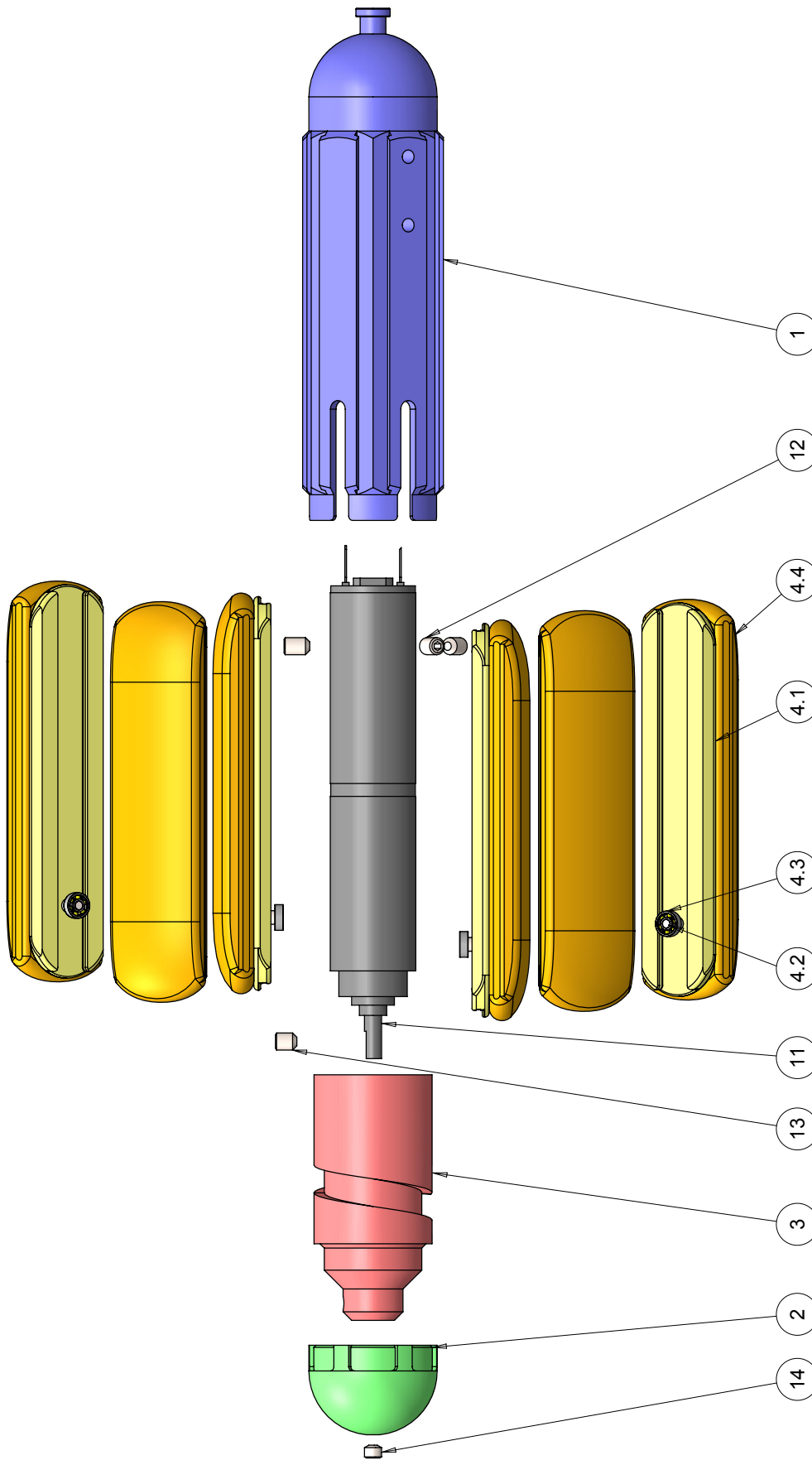
This appendix contains the production drawings that were used to manufacture the physical prototype. The first two pages contain an overview and exploded view of the total assembly, the following pages contain the production drawings of the individual parts.

ITEM NO.	PART NUMBER	Material/note	QTY.
1	1 Housing bottom extra motor mounting holes	Bronze	1
2	2 Housing top	Aluminium 7075	1
3	3 Rotor	Aluminium 7075	1
4	4 Slider with bearing	Sub assembly	6
5	5 Motor Gearhead assembly	Buy from Maxon	1
6	ISO 4026 M2 x 3N		3
7	ISO 4026 M2 x 2.5N		1
8	ISO 4026 M2 x 1.5N		1



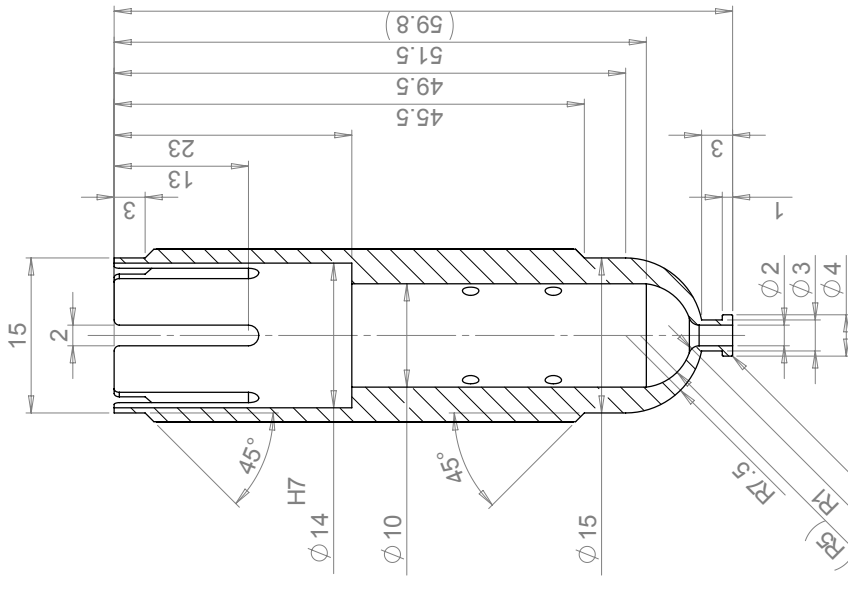
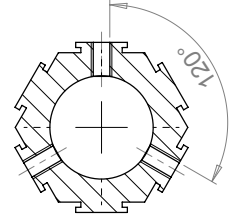
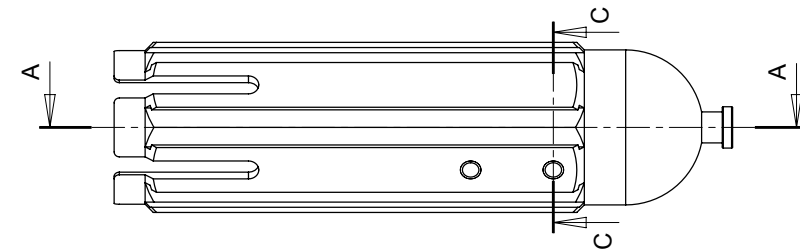
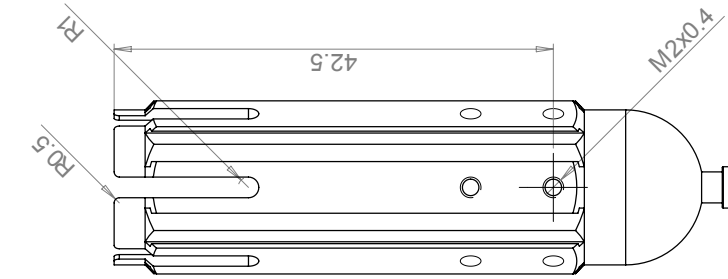
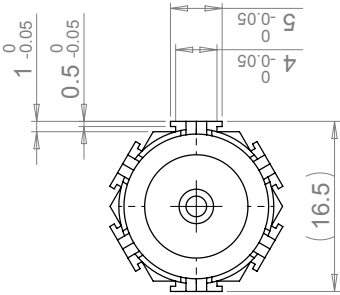
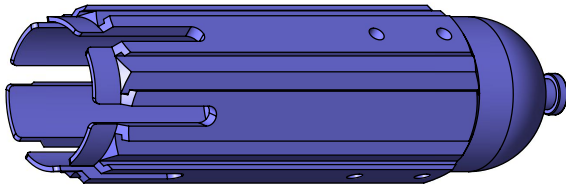
SECTION C C

ROUGHNESS 3.2	MATERIAL:	FINISH:	MASS [g]:	GEN.TOL: QTY: REV.:
THIRD ANGLE PROJECTION	SCALE: 2:1	DRAWN BY: Perry Posthoorn	±0.05 1	
	DIMENSIONS: mm	DESIGN BY: Perry Posthoorn	Drawing No: 0	
	DATE: 14/12/2016	PROJECT:		
TU Delft Perry Posthoorn posthoorn@gmail.com		NAME / DESCRIPTION: 0 Main assembly		
		A3		



- 2 clamps inside 1
- 3 rotates freely inside 1
- 4.1 slides freely over 1
- 4.2 is glued in 4.1
- 4.3 is glued on 4.2

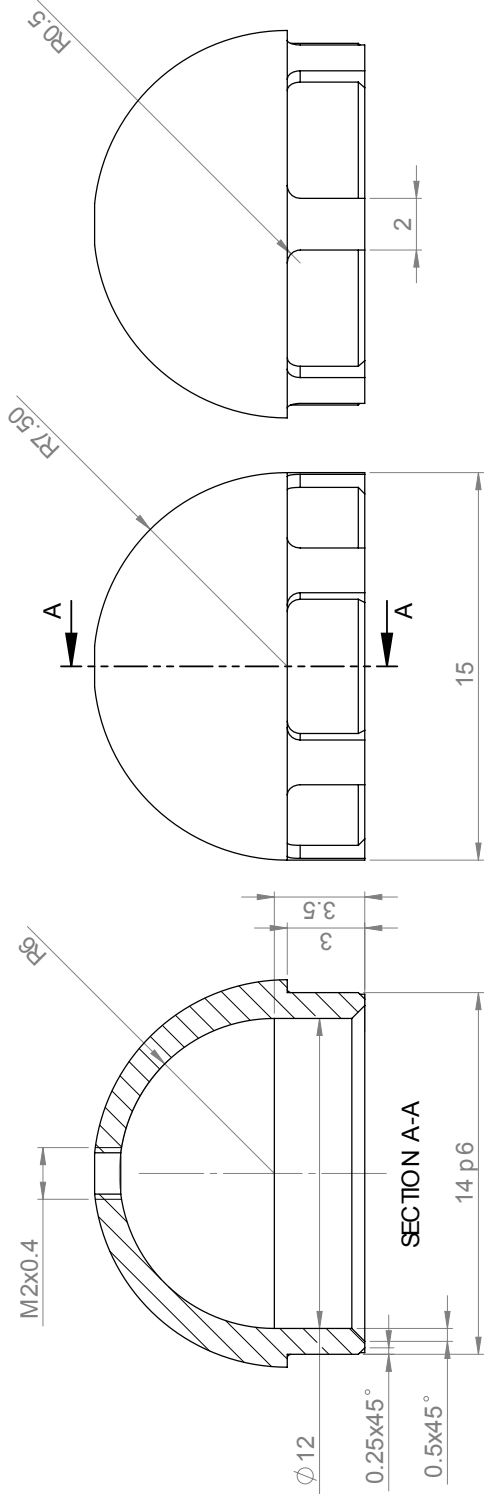
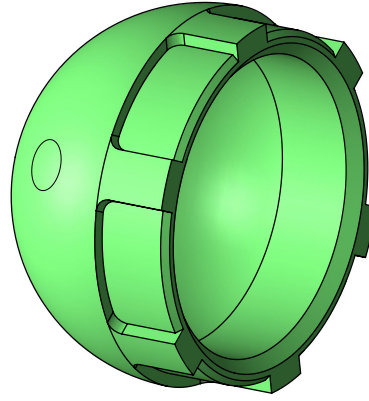
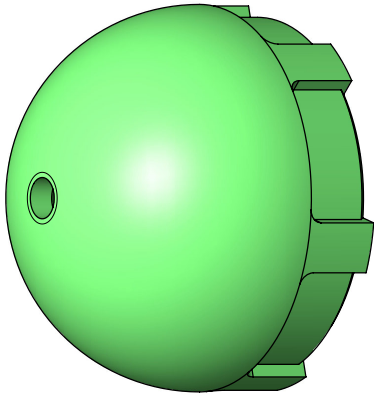
ROUGHNESS: 3.2	MATERIAL:	FINISH:	MASS(g):	GEN.TOL: ±0.05	QTY: 1	REV.:
THIRD ANGLE PROJECTION	SCALE: 2:1	DRAWN BY: Perry Posthoorn	Drawing No:			
	DIMENSIONS: mm	DESIGN BY: Perry Posthoorn	PROJECT: 0.1			
	DATE: 14122016	NAME / DESCRIPTION:				
 Perry Posthoorn pposthoorn@gmail.com		0 Main assembly exploded view A3				



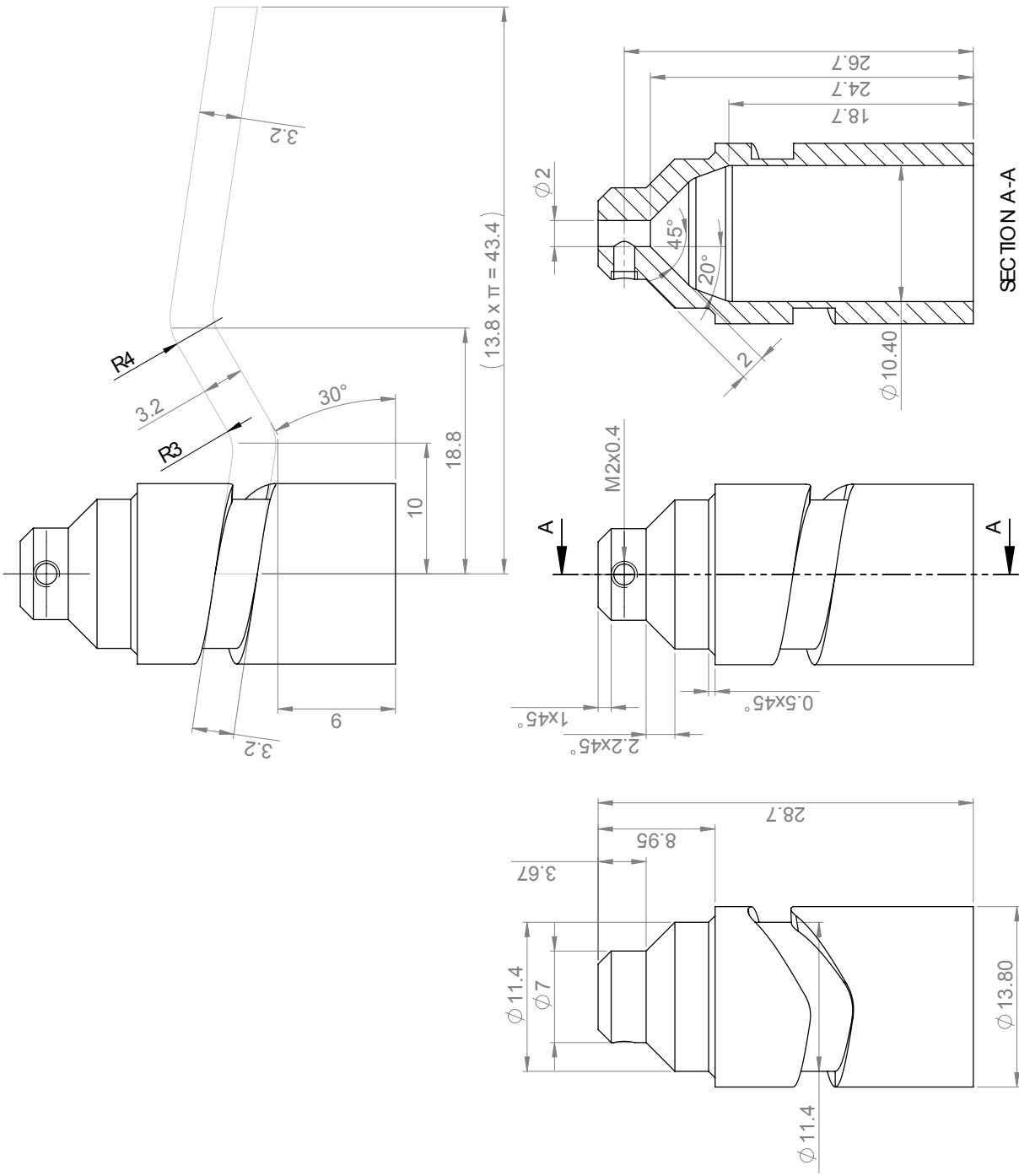
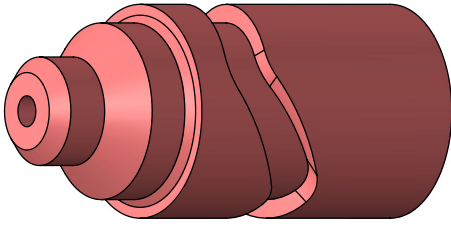
SECTION A-A

SECTION C-C

ROUGHNESS: 3.2	MATERIAL: Bronze	FINISH:	MASS(g):	GEN.TOL: ± 0.05	QTY: 1	REV.:
THIRD ANGLE PROJECTION	SCALE: 2:1	DRAWN BY: Pery Posthoorn	DRAWING No:			
	DIMENSIONS: mm	DESIGN BY: Pery Posthoorn	PROJECT: 1			
	DATE: 14-12-2016	NAME / DESCRIPTION:				
TU Delft		1 Housing bottom				
Pery Posthoorn						
pposthoorn@gmail.com						



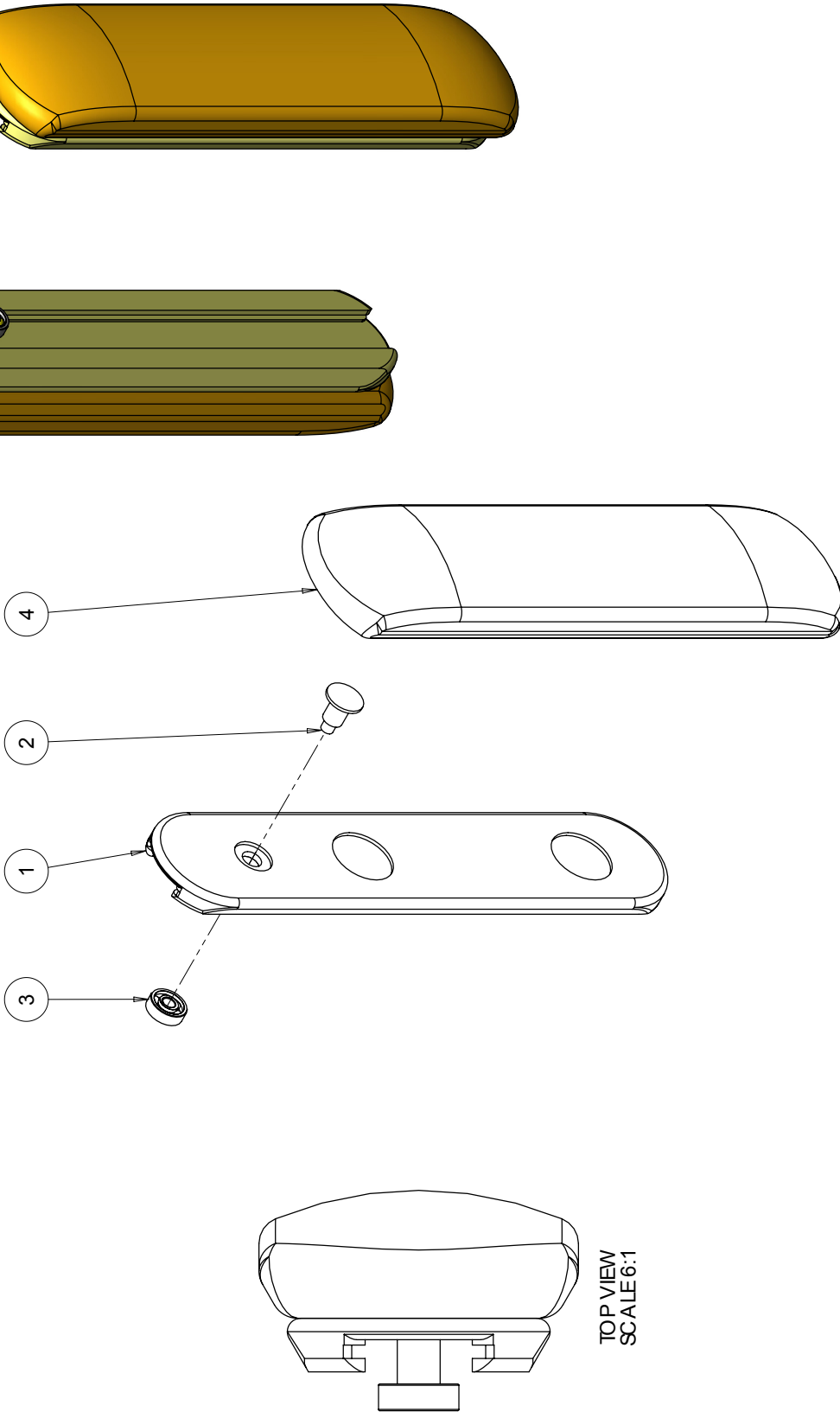
ROUGHNESS:	MATERIAL:	FINISH:	MASS(g):	GEN.TOL:	QTY:	REV.:
	Aluminium 7075			±0.05	1	
THIRD ANGLE PROJECTION	SCALE:	DRAWN BY:	Drawing No.:			
	5:1	Perry Posthoorn	2			
	DIMENSIONS:	DESIGN BY:	PROJECT:			
	mm	Perry Posthoorn				
	DATE:	NAME / DESCRIPTION:				
	14-12-2016	2 Housing top				
 Perry Posthoorn pposthoorn@gmail.com		A3				



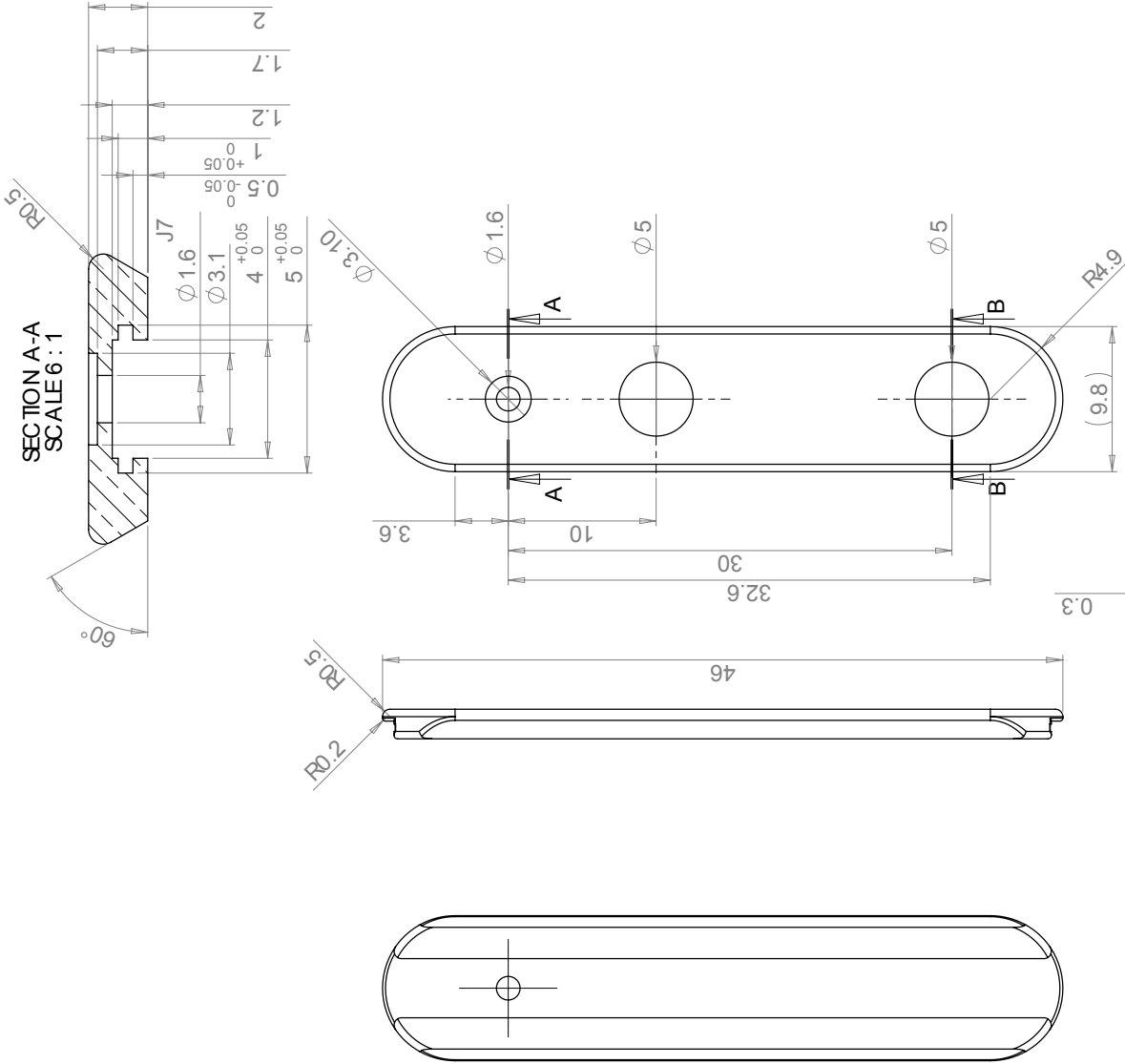
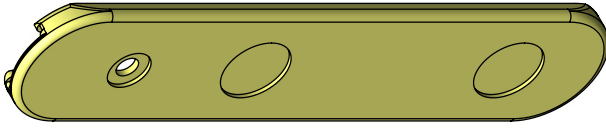
SECTION A-A

ROUGHNESS	MATERIAL: Aluminium 7075	FINISH:	MASS(g):	GEN.TOL: ±0.05	QTY: 1	REV.:
THIRD ANGLE PROJECTION	SCALE: 3:1	DRAWN BY: Pery Posthoorn	Drawing No:			
	DIMENSIONS: mm	DESIGN BY: Pery Posthoorn	PROJECT: 3			
	DATE: 14-12-2016	NAME / DESCRIPTION: 3 Rotor				
 Pery Posthoorn pposthoorn@gmail.com		A3				

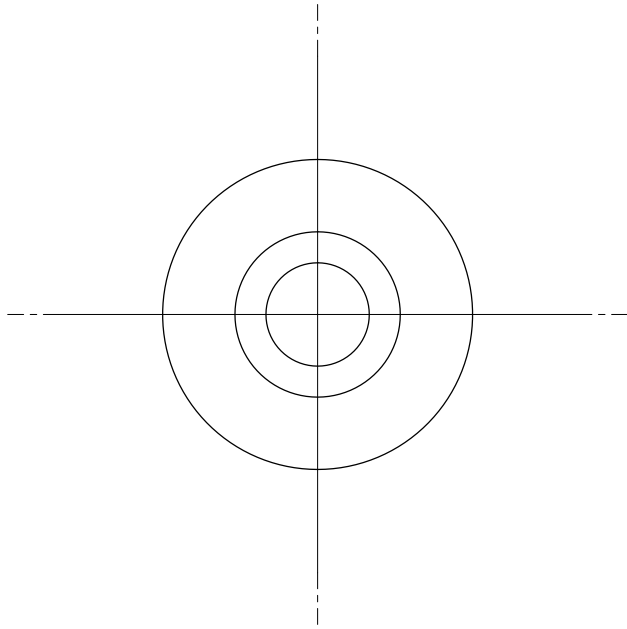
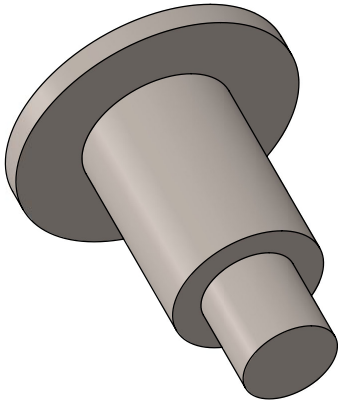
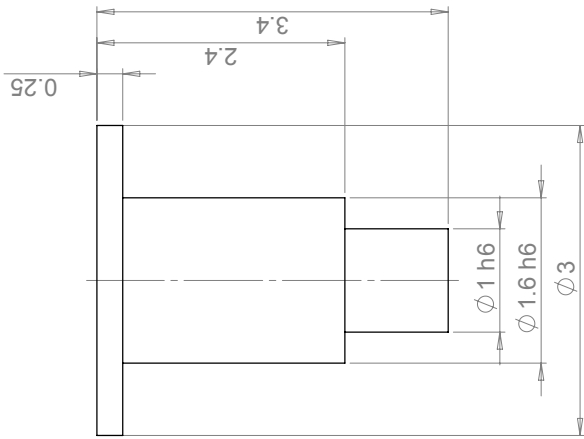
ITEM NO.	PARTNUMBER	Material/note	QTY.
1	4.1 Slider	Aluminium 7075	1
2	4.2 Slider bearing axle	Aluminium 7075	1
3	4.3 SKF_Bearing_3-1-1mm_W618_1	Buy from SKF	1
4	6 Slider texture NEW	3D Printed D1	1



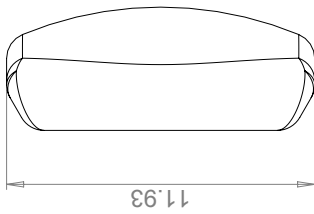
ROUGHNESS: 3.2	MATERIAL:	FINISH:	MASS(g):	GEN.TOL: ±0.05	QTY.: 18	REV.:
THIRD ANGLE PROJECTION	SCALE: 3:1	DRAWN BY: Perry Posthoorn	DRAWING No:			
	DIMENSIONS: mm	DESIGN BY: Perry Posthoorn	PROJECT: 4			
	DATE: 14-12-2016	NAME / DESCRIPTION:				
 Perry Posthoorn posthoorn@gmail.com		4 Slider with bearing subassembly A3				



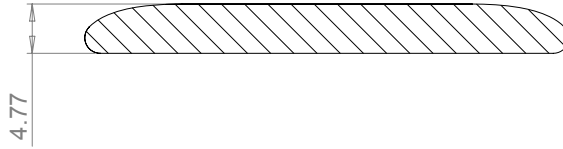
ROUGHNESS: 3.2	MATERIAL: Aluminium 7075	FINISH:	MASS(g):	GEN.TOL: ±0.05	QTY: 18	REV.:
THIRD ANGLE PROJECTION	SCALE: 3:1	DRAWN BY: Perty Posthoorn	DRAWING No:	5		
	DIMENSIONS: mm	DESIGN BY: Perty Posthoorn	PROJECT:	5		
	DATE: 14-12-2016	NAME / DESCRIPTION:				
 Perty Posthoorn pposthoorn@gmail.com		4.1 Slider				
						A3



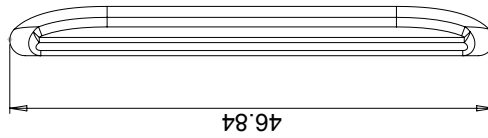
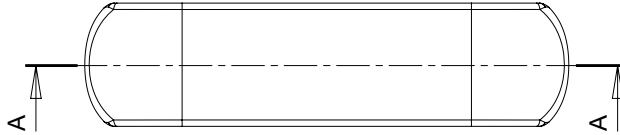
ROUGHNESS: 3.2	MATERIAL: Aluminium 7075	FINISH:	MASS(g):	GEN.TOL.: 0.05	QTY.: 18	REV.:
THIRD ANGLE PROJECTION	SCALE: 20:1	DRAWN BY: Pery Posthoorn	DRAWING No:	0.05		
	DIMENSIONS: mm	DESIGN BY: Pery Posthoorn	PROJECT: 6	Drawing No:		
	DATE: 14-12-2016	PROJECT:	NAME / DESCRIPTION:			
		Pery Posthoorn pposthoorn@gmail.com				
			4.2 Slider bearing axle			
			A3			



Scale 5:1



SECTION A-A



ROUGHNESS: 3.2	MATERIAL:	FINISH:	MASS(g):	GEN.TOL:	QTY:	REV.:
THIRD ANGLE PROJECTION	SCALE: 2:1	DRAWN BY: Perry Posthoorn	±0.1	Drawing No:		
	DIMENSIONS: mm	DESIGN BY: Perry Posthoorn				
	DATE: 14-12-2016	PROJECT:				
		NAME / DESCRIPTION:				
Perry Posthoorn posthoorn@gmail.com		6 Slider texture				
						A3